RSC Advances

PAPER

View Article Online
View Journal | View Issue

Check for updates

Cite this: *RSC Adv.*, 2023, **13**, 15810

New 1,3,4-thiadiazoles as potential anticancer agents: pro-apoptotic, cell cycle arrest, molecular modelling, and ADMET profile†

Mohamed H. Hekal,[a] Paula S. Farag,[a] Magdy M. Hemdan,[a] Amira A. El-Sayed,[a] Aya I. Hassaballah[a] and Wael M. El-Sayed*[b]

A series of novel 1,3,4-thiadiazoles was synthesized *via* the reaction of *N*-(5-(2-cyanoacetamido)-1,3,4-thiadiazol-2-yl)benzamide (**3**) with different carbon electrophiles and evaluated as potential anticancer agents. The chemical structures of these derivatives were fully elucidated using various spectral and elemental analyses. Out of 24 new thiadiazoles, derivatives **4**, **6b**, **7a**, **7d**, and **19** have significant antiproliferative activity. However, derivatives **4**, **7a**, and **7d** were toxic to the normal fibroblasts, and therefore were excluded from further investigations. Derivatives **6b** and **19** with IC_{50} at less than 10 μM and with high selectivity were selected for further studies in breast cells (MCF-7). Derivative **19** arrested the breast cells at G2/M probably through inhibition of CDK1, while **6b** significantly increased the sub-G1 percent of cells probably through induction of necrosis. These results were confirmed by the annexin V-PI assay where **6b** did not induce apoptosis and increased the necrotic cells to 12.5%, and compound **19** significantly increased the early apoptosis to 15% and increased the necrotic cells to 15%. Molecular docking showed that compound **19** was like **FB8**, an inhibitor of CDK1, in binding the CDK1 pocket. Therefore, compound **19** could be a potential CDK1 inhibitor. Derivatives **6b** and **19** did not violate Lipinski's rule of five. *In silico* studies showed that these derivatives have a low blood–brain barrier penetration capability and high intestinal absorption. Taken together, derivatives **6b** and **19** could serve as potential anticancer agents and merit further investigations.

Received 24th April 2023
Accepted 11th May 2023

DOI: 10.1039/d3ra02716c

rsc.li/rsc-advances

Open Access Article. Published on 25 May 2023. Downloaded on 2/11/2026 2:26:17 AM.
This article is licensed under a Creative Commons Attribution-NonCommercial 3.0 Unported Licence.

1. Introduction

Heterocyclic compounds are key structural moieties in several anticancer drugs. According to the FDA, most novel molecular anticancer agents contain heterocyclic rings within their structures.[1] Due to their adaptability, heterocycle-based drugs can easily target various metabolic pathways and cellular processes in cancer pathology.[2] Various heterocyclic compounds have been synthesized and reported for their potential applications as therapeutic agents. Among these compounds, the five-membered heterocyclic scaffolds, oxadiazoles, triazoles, and thiadiazoles are the most significant compounds. Thiadiazoles have been reported to exhibit several biological activities. Among the thiadiazole isomers, 1,3,4-derivatives showed preferable metabolic stability and availability.[3] This is the most promising moiety with different therapeutic activities such as anticancer,[4] antiviral,[5] anti-inflammatory,[6] antidiabetic activity,[7] and antidepressant activity.[8]

The interesting pharmacological properties of 1,3,4-thiadiazoles is attributed to their high aromaticity, *in vivo* stability, and lack of toxicity.[9] Moreover, the capability of the hydrogen binding domain allows the use of 1,3,4-thiadiazole as one of the potential agents in many FDA-approved[10] drugs such as desaglybuzole, acetazolamide, sulfamethizole, litronesib, filanesib, and methazolamide[11] (Fig. 1).

The present study aimed at synthesizing new thiadiazole derivatives and investigating the antiproliferative effect on various human cell lines as well as investigating the possible mechanism(s) of action through assessing the effect of these derivatives on cell cycle and apoptosis by flow cytometry. Different *in silico* and docking studies were performed to predict some of the pharmacological characteristics of the new thiadiazoles.

2. Experimental

2.1 Chemistry

All melting points were determined using uncorrected Griffin and George melting-point equipment (Griffin & George Ltd.,

[a]*Department of Chemistry, Faculty of Science, Ain Shams University, Abbassia, 11566 Cairo, Egypt*

[b]*Department of Zoology, Faculty of Science, Ain Shams University, Abbassia, 11566 Cairo, Egypt. E-mail: waelelhalawany@hotmail.com; wael_farag@sci.asu.edu.eg; Fax: +202 2684 2123; Tel: +202 2482 1633*

† Electronic supplementary information (ESI) available. See DOI: https://doi.org/10.1039/d3ra02716c

© 2023 The Author(s). Published by the Royal Society of Chemistry

Open Access Article. Published on 25 May 2023. Downloaded on 2/11/2026 2:26:17 AM.
This article is licensed under a Creative Commons Attribution-NonCommercial 3.0 Unported Licence.

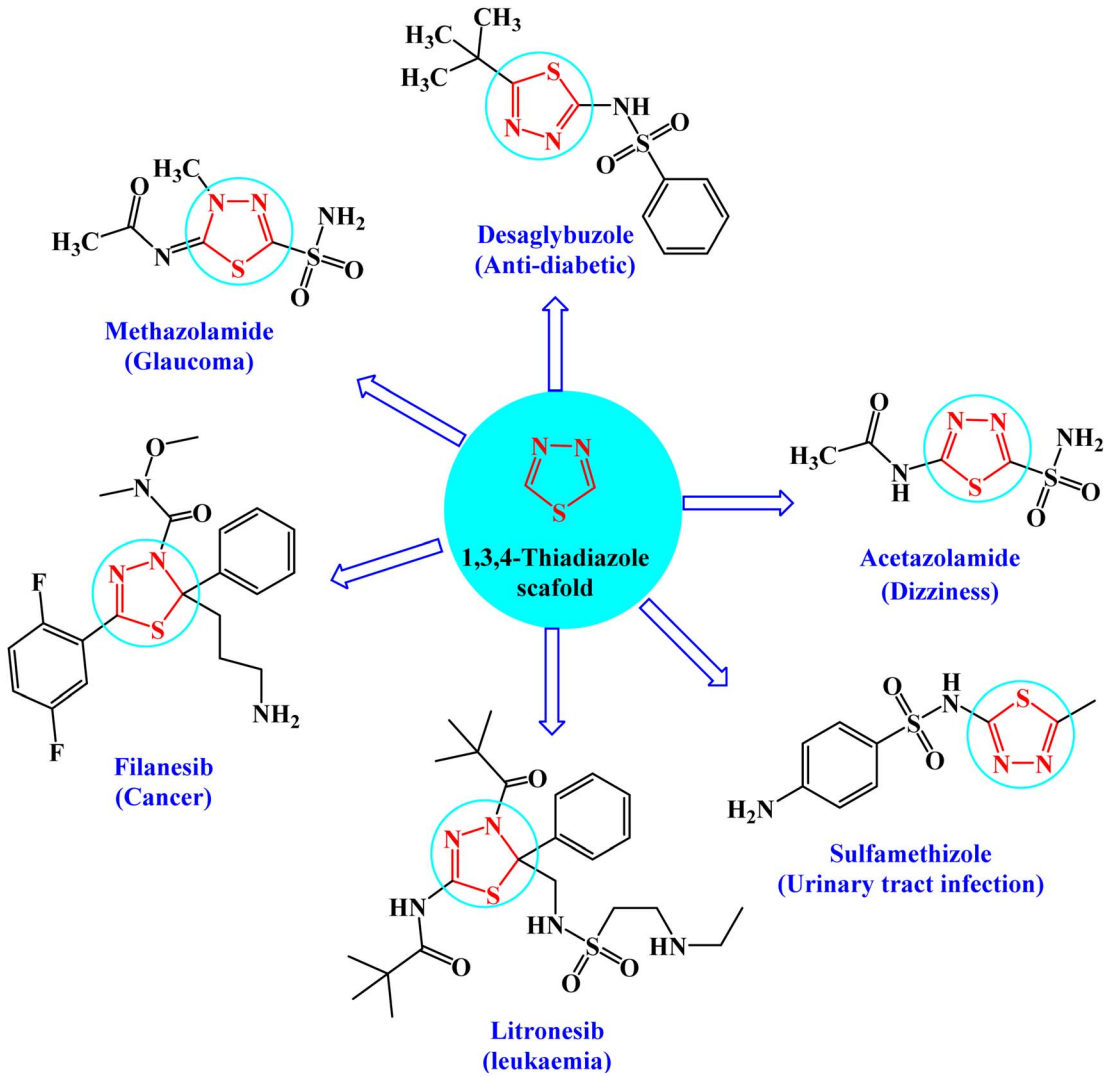

Fig. 1 FDA-approved drugs of 1,3,4-thiadiazole derivatives showing their common pharmacophoric features.

Wembley, Middlesex, UK). The quality of the produced compounds was controlled using aluminum sheet silica gel F_{254} (Merck) thin layer chromatography (TLC). The KBr wafer approach was used to record IR-spectra using a Pye Unicam SP1200 spectrophotometer (Pye Unicam Ltd., Cambridge, UK). ^{1}H-NMR spectra were obtained on a Bruker Avance (III) utilizing a Varian-Gemini 400 MHz and an internal standard of tetramethyl silane (chemical shifts in scale δ_{ppm}), whereas ^{13}C-NMR spectra were obtained at 100 MHz. In deuterated dimethyl sulfoxide, TMS was used as an internal standard (DMSO-d_6). Chemical changes were described as elemental studies were performed using a PerkinElmer 2400 CHN elemental analyzer at the Microanalytical Unit, Faculty of Science, Ain Shams University, and satisfactory analytical data (±0.4) were obtained for all derivatives.

2.1.1 *N*-(5-Amino-1,3,4-thiadiazol-2-yl)benzamide (2). Method (I): a solution of *N*-(2-carbamothioylhydrazine-1-carbonothioyl)benzamide (**1**) (2.5 g, 10 mmol) in acetic acid (15 mL) was refluxed for three hours. The deposited solid while heating was filtered off and then recrystallized from acetic acid affording the pure compound **2** as yellow crystals; (2.1 g, 91%); m.p. 278–280 °C; IR (KBr) (υ_{max}, cm^{-1}): 3448, 3446 (NH_2), 3164 (NH), 3060 (CH aromatic), 1672, 1638 (C=O), 1601 (C=N). Anal. calcd for $C_9H_8N_4OS$ (220.25) C, 49.08; H, 3.66; N, 25.44; found: C, 49.18; H, 3.63; N, 25.60.

Method (II): a mixture of *N*-(2-carbamothioylhydrazine-1-carbonothioyl)benzamide (**1**) (2.5 g, 10 mmol) and sulfuric acid 98% (10 mL) was stirred at room temperature for 1.5 h, kept in refrigerator overnight, and then poured onto cold water. The precipitated solid was separated by filtration, dried, and recrystallized from *N*,*N*-dimethyl formamide affording the pure compound **2** as yellow crystals; (1.1 g, 50%) (identity m.p., TLC, and IR).

2.1.2 *N*-(5-(2-Cyanoacetamido)-1,3,4-thiadiazol-2-yl) benzamide (3). A mixture of compound **2** (2.2 g, 10 mmol) and ethyl cyanoacetate (1.13 mL, 10 mmol) with a catalytic amount of TEA was stirred in 10 mL of absolute ethanol for three hours. The reaction mixture was acidified by cold dilute HCl, the

Open Access Article. Published on 25 May 2023. Downloaded on 2/11/2026 2:26:17 AM. This article is licensed under a Creative Commons Attribution-NonCommercial 3.0 Unported Licence.

deposited solid was filtered off and recrystallized from EtOH/dioxane [1 : 3] giving the pure compound **3** as yellow crystals; (2.1 g, 75%); m.p. 204–206 °C; IR (KBr) (υ_{max}, cm^{-1}): 3213 (NH), 3080 (CH aromatic), 2918, 2894 (CH aliphatic), 2257 (C≡N), 1691, 1673 (C=O), 1612 (C=N). ^{1}H-NMR (300 MHz, DMSO-d_6) δ_{ppm}: 3.88 (s, 2H, CH_2), 7.46–7.95 (m, 5H, ArH), 11.69 (br s, 1H, $CH_2CO\underline{NH}$, exchangeable with D_2O), 12.59 (br s, 1H, $PhCO\underline{NH}$, exchangeable with D_2O). ^{13}C-NMR (100 MHz, DMSO-d_6) δ_{ppm}: 24.06, 115.46, 115.60, 128.53, 128.84, 131.83, 133.30, 160.11, 166.58, 167.40, 168.10, 178.14. Anal. calcd for $C_{12}H_9N_5O_2S$ (287.30) C, 50.17; H, 3.16; N, 24.38; found: C, 50.27; H, 3.01; N, 24.30.

2.1.3 *N*-(5-Benzamido-1,3,4-thiadiazol-2-yl)-2-imino-2*H*-chromene-3-carboxamide (4). A mixture of compound **3** (2.8 g, 10 mmol) and salicylaldehyde (1.2 mL, 10 mmol) with a catalytic amount of piperidine in absolute ethanol 10 mL was heated under reflux for three hours. The deposited solid while heating was collected by filtration, dried, and recrystallized from dioxane producing **4** as orange crystals; (3.5 g, 84%); m.p. 240–242 °C; IR (KBr) (υ_{max}, cm^{-1}): 3409, 3158 (NH), 3060, 3044 (CH aromatic), 2971 (CH aliphatic), 1679 (C=O), 1636 (C=N). ^{1}H-NMR (300 MHz, DMSO-d_6) δ_{ppm}: 7.28–8.00 (m, 9H, ArH), 8.58 (s, 1H, C=CH olefinic), 11.76 (br s, 1H, C = $\underline{NH}$, exchangeable with D_2O), 13.98 (br s, 2H, $2\underline{NH}CO$, exchangeable with D_2O). ^{13}C-NMR (100 MHz, DMSO-d_6) δ_{ppm}: 115.41, 118.12, 118.50, 124.71, 128.58 (2C), 128.70, 128.86, 129.40, 130.40, 131.94, 133.01, 133.27, 133.78, 142.42, 153.24, 156.25, 156.80, 168.39. Anal. calcd for $C_{19}H_{13}N_5O_3S$ (391.41) %: C, 58.31; H, 3.35; N, 17.89; found: C, 58.28; H, 3.38; N, 17.70.

The filtrate was acidified by cold dilute HCl. The deposited solid was filtered out, dried, and recrystallized from EtOH/dioxane [3 : 1] affording compound **5**.

2.1.4 *N*-(5-Benzamido-1,3,4-thiadiazol-2-yl)-2-oxo-2*H*-chromene-3-carboxamide (5). Yellow crystals; (3 g, 78%); m.p. > 300 °C; IR (KBr) (υ_{max}, cm^{-1}): 3221, 3179 (NH), 3038 (CH aromatic), 1713 ($C=O_{lactone}$), 1679, 1655 ($C=O_{amide}$), 1608 (C=N). ^{1}H-NMR (400 MHz, DMSO-d_6) δ_{ppm}: 7.48–7.57 (m, 5H, ArH), 7.66 (d, J = 7.24 Hz, 1H, ArH), 7.79 (d, J = 7.76 Hz, 1H, ArH), 8.00–8.08 (m, 2H, ArH), 9.04 (s, 1H, C=CH olefinic), 12.20 (br s, 1H, NH, exchangeable with D_2O), 13.74 (br s, 1H, NH, exchangeable with D_2O). ^{13}C-NMR (100 MHz, DMSO-d_6) δ_{ppm}: 104.51, 116.56, 117.96, 120.23, 123.32, 123.76, 126.28 (2C), 128.58, 130, 131.67, 134.63, 140.30 (2C), 152.43 (2C), 166.99 (2C), 169.65. Anal. calcd for $C_{19}H_{12}N_4O_4S$ (392.39) %: C, 58.16; H, 3.08; N, 14.28; found: C, 58.20; H, 3.10; N, 14.25.

2.1.5 *N*-(5-(6-amino-4-argio-3,5-dicyano-2-oxopyridin-1(2*H*)-yl)-1,3,4-thiadiazol-2-yl)benzamide (6a). A mixture of compound **3** (2.8 g, 10 mmol) and 2-(4-methoxy-benzylidene) malononitrile "arylidene" (1.8 g, 10 mmol) with a catalytic amount of piperidine was refluxed in absolute ethanol 10 mL for 4.5 h. The precipitated crystals were filtered off and washed with boiling ethanol affording compound **6a** as gray crystals; (3.3 g, 73%); m.p. > 300 °C; IR (KBr) (υ_{max}, cm^{-1}): 3455, 3394 (NH_2), 3263 (NH), 3099 (CH aromatic), 2944, 2844 (CH aliphatic), 2219 (C≡N), 1660, 1641 (C=O). ^{1}H-NMR (400 MHz, DMSO-d_6) δ_{ppm}: 3.88 (s, 3H, OCH_3), 5.59 (s, 2H, NH_2, exchangeable with D_2O), 7.18 (d, J = 8.80 Hz, 2H, ArH), 7.54 (t, J = 7.76 Hz, 2H, ArH), 7.67 (t, J = 7.4 Hz, 1H, ArH), 7.97–8.22 (m, 4H, ArH), 12.42 (br s, 1H, $\underline{NH}CO$, exchangeable with D_2O). ^{13}C-NMR (100 MHz, DMSO-d_6) δ_{ppm}: 66.13, 71.23, 116.39, 117.57, 121.90, 123.72, 124.02, 124.39, 126.28, 127.08 (2C), 127.74, 129.80, 130.83, 132.22, 135.78, 147.67, 152.57, 153.56, 153.81, 162.56, 170.13, 170.20. Anal. calcd for $C_{23}H_{15}N_7O_3S$ (469.48) %: C, 58.84; H, 3.22; N, 20.88; found: C, 58.80; H, 3.28; N, 20.82.

The reaction filtrate was poured onto ice cold dilute HCl with stirring. The crude material was filtered off and recrystallized from dioxane giving **6b**.

2.1.6 *N*-(5-(2-Cyano-3-(4-methoxyphenyl)acrylamido)-1,3,4-thiadiazol-2-yl)benzamide (6b). Orange crystals; (2.6 g, 65%); m.p. 252–254 °C; IR (KBr) (υ_{max}, cm^{-1}): 3233 (NH), 3066, 3020 (CH aromatic), 2984, 2935 (CH aliphatic), 2207 (C≡N), 1681 (C=O). ^{1}H-NMR (400 MHz, DMSO-d_6) δ_{ppm}: 3.88 (s, 3H, OCH_3), 7.18 (d, J = 8.80 Hz, 2H, ArH), 7.54 (t, J = 7.76 Hz, 2H, ArH), 7.67 (t, J = 7.4 Hz, 1H, ArH), 7.97–8.04 (m, 4H, ArH), 8.22 (s, 1H, $=CH_{olefinic}$), 11.11 (br s, 1H, NH, exchangeable with D_2O), 11.81 (br s, 1H, NH, exchangeable with D_2O). ^{13}C-NMR (100 MHz, DMSO-d_6) δ_{ppm}: 20.58, 55.62, 112.29 (2C), 114.63 (2C), 118.80, 127.50 (2C), 128.99 (2C), 129.53 (2C), 137.06 (2C), 146.06 (2C), 159.78, 170.44, 178.66. Anal. calcd for $C_{20}H_{15}N_5O_3S$ (405.43) %: C, 59.25; H, 3.73; N, 17.27; found: C, 59.30; H, 3.70; N, 17.30.

2.1.7 General procedure for the synthesis of compounds (7a–f). A mixture of compound **3** (2.8 g, 10 mmol) and the appropriate aldehyde derivatives namely; 2,4-dichlorobenzaldehyde (1.7 g, 10 mmol), *p*-chlorobenzaldehyde (1.4 g, 10 mmol), furan-2-carbaldehyde (0.96 mL, 10 mmol), thiophene-2-carbaldehyde (1.2 mL, 10 mmol), *p*-nitrobenzaldehyde (1.5 g, 10 mmol), or 4-hydroxy-3-methoxybenzaldehyde (1.5 g, 10 mmol) in absolute ethanol (10 mL) in the presence of a catalytic amount of piperidine was refluxed for three hours. The precipitated crystals were filtered off and recrystallized from ethanol affording compounds **7a–f**.

2.1.8 *N*-(5-(2-Cyano-3-(2,4-dichlorophenyl)acrylamido)-1,3,4-thiadiazol-2-yl)benzamide (7a). Yellow crystals; (3.1 g, 72%); m.p. > 300 °C; IR (KBr) (υ_{max}, cm^{-1}): 3197, 3154 (NH), 3095, 3069, 3019 (CH aromatic), 2921 (CH aliphatic), 2229 (C≡N), 1660 ($C=O_{amide}$). ^{1}H-NMR (400 MHz, DMSO-d_6) δ_{ppm}: 7.57–8.17 (m, 8H, ArH), 8.29 (s, 1H, $=CH_{olefinic}$), 12.72 (br s, 1H, NH, exchangeable with D_2O), 13.47 (br s, 1H, NH, exchangeable with D_2O). ^{13}C-NMR (100 MHz, DMSO-d_6) δ_{ppm}: 103.93, 112.94, 115.85, 117.93, 129.74 (2C), 131.93 (2C), 132.04, 136.85 (2C), 146.12, 146.39, 148.22, 156.91, 159.10, 160.49, 170.08, 170.69. Anal. calcd for $C_{19}H_{11}Cl_2N_5O_2S$ (444.29) %: C, 51.36; H, 2.50; Cl, 15.96; N, 15.76; found: C, 51.30; H, 2.43; Cl, 15.89; N, 15.80.

2.1.9 *N*-(5-(3-(4-Chlorophenyl)-2-cyanoacrylamido)-1,3,4-thiadiazol-2-yl)benzamide (7b). Orange crystals; (3.2 g, 80%); m.p. 258–260 °C; IR (KBr) (υ_{max}, cm^{-1}): 3237 (NH_{br}), 3056 (CH aromatic), 2970 (CH aliphatic), 2212 (C≡N), 1686, 1665 ($C=O_{amide}$). ^{1}H-NMR (400 MHz, DMSO-d_6) δ_{ppm}: 7.53–8.02 (m, 9H, ArH), 8.29 (s, 1H, $=CH_{olefinic}$), 11.28 (br s, 1H, $\underline{NH}CO$, exchangeable with D_2O), 12.40 (br s, 1H, $CO\underline{NH}$, exchangeable with D_2O). ^{13}C-NMR (100 MHz, DMSO-d_6) δ_{ppm}: 68.28, 70.01, 120.90, 123.02, 123.13, 125.59, 126.03, 126.71, 127, 128.11, 128.46, 128.55, 129.80, 129.89, 135.19, 146.74, 167.69, 170.62, 170.77. Anal. calcd for $C_{19}H_{12}ClN_5O_2S$ (409.85) %: C, 55.68; H,

© 2023 The Author(s). Published by the Royal Society of Chemistry

Open Access Article. Published on 25 May 2023. Downloaded on 2/11/2026 2:26:17 AM. This article is licensed under a Creative Commons Attribution-NonCommercial 3.0 Unported Licence.

2.95; Cl, 8.65; N, 17.09; found: C, 55.70; H, 2.98; Cl, 8.72; N, 17.15.

2.1.10 *N*-(5-(2-Cyano-3-(furan-2-yl)acrylamido)-1,3,4-thiadiazol-2-yl)benzamide (7c). White crystals; (3.4 g, 95%); m.p. 276–278 °C; IR (KBr) (υ_{max}, cm^{-1}): 3291, 3238 (NH), 3067, 3040 (CH aromatic), 2215 (C≡N), 1684, 1664 (C=O_{amide}), 1614 (C=N). ^{1}H-NMR (400 MHz, DMSO-d_6) δ_{ppm}: 6.87–6.88 (m, 1H, ArH), 7.48–7.56 (m, 4H, ArH), 7.67 (t, J = 7.36 Hz, 2H, ArH), 7.97–8.08 (m, 1H, ArH), 8.20 (s, 1H, =$CH_{olefinic}$), 11.82 (br s, 1H, NH CO, exchangeable with D_2O), 12.43 (br s, 1H, CONH, exchangeable with D_2O). ^{13}C-NMR (100 MHz, DMSO-d_6) δ_{ppm}: 102.91, 117.04, 118.04, 121.51, 124.32, 124.76, 127.11 (2C), 129.58 (2C), 131.00, 132.67, 135.63, 141.39, 153.43, 167.98, 170.65. Anal. calcd for $C_{17}H_{11}N_5O_3S$ (365.37) %: C, 55.89; H, 3.03; N, 19.17; found: C, 55.93; H, 3.10; N, 19.15.

2.1.11 *N*-(5-(2-Cyano-3-(thiophen-2-yl)acrylamido)-1,3,4-thiadiazol-2-yl)benzamide (7d). Gray crystals; (3.2 g, 85%); m.p. 268–270 °C; IR (KBr) (υ_{max}, cm^{-1}): 3244 (NH), 3098, 3018 (CH aromatic), 2924 (CH aliphatic), 2209 (C≡N), 1687, 1667 (C=O_{amide}). ^{1}H-NMR (400 MHz, DMSO-d_6) δ_{ppm}: 7.36 (t, J = 8.76 Hz, 1H, ArH), 7.54 (t, J = 7.84 Hz, 2H, ArH), 7.67 (t, J = 7.4 Hz, 1H, ArH), 7.97–7.99 (m, 3H, ArH), 8.18 (d, J = 4.96 Hz, 1H, ArH), 8.52 (s, 1H, =$CH_{olefinic}$), 11.82 (br s, 1H, NH CO, exchangeable with D_2O), 12.41 (br s, 1H, CONH, exchangeable with D_2O). ^{13}C-NMR (100 MHz, DMSO-d_6) δ_{ppm}: 109.22, 119.18 (2C), 120.67, 123.35, 126.23, 126.67, 129.11, 131.85, 133.27, 134.76, 137.48, 143.22, 155.37 (2C), 169.99, 172.42. Anal. calcd for $C_{17}H_{11}N_5O_2S_2$ (381.43) %: C, 53.53; H, 2.91; N, 18.36; found: C, 53.58; H, 2.80; N, 18.25.

2.1.12 *N*-(5-(2-Cyano-3-(4-nitrophenyl)acrylamido)-1,3,4-thiadiazol-2-yl)benzamide (7e). Yellow crystals; (3.0 g, 73%); m.p. > 300 °C; IR (KBr) (υ_{max}, cm^{-1}): 3203, 3154 (NH), 3068, 3053 (CH aromatic), 2936 (CH aliphatic), 2233 (C≡N), 1669 (C=O). ^{1}H-NMR (400 MHz, DMSO-d_6) δ_{ppm}: 7.59 (t, J = 7.32 Hz, 2H, ArH), 7.69 (t, J = 7.2 Hz, 1H, ArH), 8.15 (d, J = 7.48 Hz, 2H, ArH), 8.25 (d, J = 8.16 Hz, 2H, ArH), 8.40–8.45 (m, 2H, ArH + 1H, =$CH_{olefinic}$), 12.55 (br s, 1H, NH, exchangeable with D_2O), 13.45 (br s, 1H, NH, exchangeable with D_2O). ^{13}C-NMR (100 MHz, DMSO-d_6) δ_{ppm}: 112.94, 113.29, 116.98, 117.83, 129.28, 129.52, 130.28 (2C), 131.05, 131.25, 134.62, 135.78, 148.16, 154.35, 160.65, 161.47, 170.82, 174.14, 174.73. Anal. calcd for $C_{19}H_{12}N_6O_4S$ (420.40) %: C, 54.28; H, 2.88; N, 19.99; found: C, 54.30; H, 2.85; N, 19.90.

2.1.13 *N*-(5-(2-Cyano-3-(4-hydroxy-3-methoxyphenyl) acrylamido)-1,3,4-thiadiazol-2-yl)benzamide (7f). Pale yellow crystals; (3.7 g, 90%); m.p. 240–242 °C; IR (KBr) (υ_{max}, cm^{-1}): 3259 (OH), 3181, 3106 (NH), 3006 (CH aromatic), 2922, 2839 (CH aliphatic), 2219 (C≡N), 1667 (C=O_{amide}). ^{1}H-NMR (400 MHz, DMSO-d_6) δ_{ppm}: 3.85 (s, 3H, OCH_3), 6.96 (d, J = 8.32 Hz, 1H, ArH), 7.56–7.78 (m, 5H, ArH), 8.11–8.15 (m, 2H, ArH + 1H, =$CH_{olefinic}$), 10.24 (br s, 1H, OH, exchangeable with D_2O), 12.07 (br s, 1H, NH, exchangeable with D_2O), 13.30 (br s, 1H, NH, exchangeable with D_2O). ^{13}C-NMR (100 MHz, DMSO-d_6) δ_{ppm}: 65.73, 66.81, 68.92, 116.04, 117.41, 120.44, 123.33, 123.69, 126.08, 128.56, 129.98, 131.66, 134.43, 140.38, 152.45, 158.87, 159.51, 166.93, 168.85, 169.66. Anal. calcd for $C_{20}H_{15}N_5O_4S$ (421.43) %: C, 57.00; H, 3.59; N, 16.62; found: C, 57.09; H, 3.62; N, 16.58.

2.1.14 General procedure for the synthesis of compounds (9 and 10). A mixture of compound **3** (2.8 g, 10 mmol) and the appropriate diketone derivatives namely acetylacetone (1.00 mL, 10 mmol) or benzoyl acetone (1.6 mL, 10 mmol) in absolute ethanol (10 mL) with a catalytic base of fused sodium acetate was refluxed for three hours. The separated solid was filtered off, dried, and recrystallized from ethanol affording compounds **9** and **10**, respectively.

2.1.15 *N*-(5-(3-Cyano-4,6-dimethyl-2-oxopyridin-1(2*H*)-yl)-1,3,4-thiadiazol-2-yl)benzamide (9). White crystals; (2.2 g, 64%); m.p. 298–300 °C; IR (KBr) (υ_{max}, cm^{-1}): 3224 (NH), 3054, 3021 (CH aromatic), 2964, 2922 (CH aliphatic), 2215 (C≡N), 1648 (C=O). ^{1}H-NMR (400 MHz, DMSO-d_6) δ_{ppm}: 3.96 (s, 3H, CH_3), 3.99 (s, 3H, CH_3), 7.54–8.11 (m, 6H, ArH), 12.87 (br s, 1H, NH, exchangeable with D_2O). ^{13}C-NMR (100 MHz, DMSO-d_6) δ_{ppm}: 21.01, 21.13, 115.85, 116.66, 120.90, 123.13, 125.59, 126.71, 127.77, 129.80, 135.19, 152.70, 161.70, 167.67, 170.77, 180.28, 182.01. Anal. calcd for $C_{17}H_{13}N_5O_2S$ (351.38) %: C, 58.11; H, 3.73; N, 19.93; found: C, 58.20; H, 3.65; N, 19.88.

2.1.16 *N*-(5-(3-Cyano-4-methyl-2-oxo-6-phenylpyridin-1(2*H*)-yl)-1,3,4-thiadiazol-2-yl)benzamide (10). White crystals; (2.4 g, 60%); m.p. > 300 °C; IR (KBr) (υ_{max}, cm^{-1}): 3258, 3174 (NH), 3067 (CH aromatic), 2970, 2934 (CH aliphatic), 2218 (C≡N), 1684 (C=O), 1649 (C=N). ^{1}H-NMR (400 MHz, DMSO-d_6) δ_{ppm}: 2.15 (s, 3H, CH_3), 7.57–8.30 (m, 11H, ArH), 13.37 (br s, 1H, NH, exchangeable with D_2O). ^{13}C-NMR (100 MHz, DMSO-d_6) δ_{ppm}: 22.83, 68.92, 116.04 (2C), 117.41, 120.44, 123.33, 123.69, 126.08 (2C), 128.56, 129.98, 131.66, 134.43, 140.38, 152.45, 158.87, 159.51, 166.93, 168.85 (2C), 169.66. Anal. calcd for $C_{22}H_{15}N_5O_2S$ (413.46) %: C, 63.91; H, 3.66; N, 16.94; found: C, 63.88; H, 3.71; N, 16.81.

2.1.17 General procedure for the synthesis of compounds (11–16). 1,3,4-Thiadiazole derivative **3** (2.8 g, 10 mmol) was added to a cold suspension of finely divided potassium hydroxide (0.56 g, 10 mmol) in DMF (15 mL) with stirring for 30 minutes. Phenyl isothiocyanate (1.35 mL, 10 mmol) was added dropwise and then the mixture was allowed to stand overnight. Ethyl chloroacetate (1.22 mL, 10 mmol), chloro acetylchloride (1.12 mL, 10 mmol), diethyl malonate (1.6 mL, 10 mmol), 1,2-dibromoethane (1.87 mL, 10 mmol), methyl iodide (1.41 mL, 10 mmol), or HCl was added dropwise, stirred at room temperature for three hours and then allowed to stand overnight. The reaction mixture was placed into ice cold dilute HCl. The separated solid was filtered, washed with water, dried, and recrystallized from the suitable solvent producing **11–16**, respectively.

2.1.18 Ethyl (*E*,*Z*)-2-((3-((5-benzamido-1,3,4-thiadiazol-2-yl) amino)-2-cyano-3-oxo-1-(phenylamino) prop-1-en-1-yl)thio) acetate (11). Brown crystals; (2.7 g, 55%); m.p. 288–290 °C; IR (KBr) (υ_{max}, cm^{-1}): 3148 (NH), 3064 (CH aromatic), 2982 (CH aliphatic), 2195 (C≡N), 1734 (C=O_{ester}), br. 1673 (C=O_{amide}), 1637 (C=N). ^{1}H-NMR (400 MHz, DMSO-d_6) δ_{ppm}: 1.19 (t, 3H, CH_2CH_3), 4.06 (q, 2H, CH_2CH_3), 4.59 (s, 2H, SCH_2CO), 6.75–6.77 (m, 5H, ArH), 7.66–8.07 (m, 5H, ArH), 11.96 (br s, 1H, NH Ph, exchangeable with D_2O), 12.85–13.05 (br s, 2H, CONH,

Open Access Article. Published on 25 May 2023. Downloaded on 2/11/2026 2:26:17 AM. This article is licensed under a Creative Commons Attribution-NonCommercial 3.0 Unported Licence.

exchangeable with D_2O). Anal. calcd for $C_{23}H_{20}N_6O_4S_2$ (508.57) %: C, 54.32; H, 3.96; N, 16.53; found: C, 54.25; H, 3.87; N, 16.59.

2.1.19 *N*-(5-(2-Cyano-2-(5-oxo-3-phenylthiazolidin-2-ylidene)acetamido)-1,3,4-thiadiazol-2-yl)benzamide (12). Red crystals; (3.0 g, 64%); m.p. > 300 °C; IR (KBr) (υ_{max}, cm^{-1}): 3210, 3154 (NH), 3061 (CH aromatic), 2922 (CH aliphatic), 2204 (C≡N), 1741 (C=O_{Ketone}), br. 1670 (C=O_{amide}). ^{1}H-NMR (400 MHz, DMSO-d_6) δ_{ppm}: 4.10 (s, 2H, $\underline{CH_2}$CO), 6.72–6.77 (m, 5H, ArH), 7.64–8.05 (m, 5H, ArH), 12.95 (br s, 1H, NH, exchangeable with D_2O), 14.69 (br s, H, NH, exchangeable with D_2O). Anal. calcd for $C_{21}H_{14}N_6O_3S_2$ (462.50) %: C, 54.54; H, 3.05; N, 18.17; found: C, 54.51; H, 3.13; N, 18.11.

2.1.20 *N*-(5-(2-Cyano-2-(4,6-dioxo-1-phenylpiperidin-2-ylidene)acetamido)-1,3,4-thiadiazol-2-yl)benzamide (13). Reddish brown crystals; (2.7 g, 58%); m.p. > 300 °C; IR (KBr) (υ_{max}, cm^{-1}): 3150 (NH), 3064 (CH aromatic), 2981 (CH aliphatic), 2206 (C≡N), 1740 (C=O_{Ketone}), 1672 (C=O_{amide}), 1638 (C=N). ^{1}H-NMR (400 MHz, DMSO-d_6) δ_{ppm}: 4.62 (s, 2H, CO$\underline{CH_2}$CO), 7.49–7.59 (m, 5H, ArH), 7.84–8.04 (m, 5H, ArH), 11.89 (br s, 1H, NH, exchangeable with D_2O), 12.50 (br s, 1H, NH, exchangeable with D_2O). Anal. calcd for $C_{22}H_{14}N_6O_4S_2$ (490.51) %: C, 53.87; H, 2.88; N, 17.13; found: C, 53.96; H, 2.94; N, 17.09.

2.1.21 *N*-(5-(2-Cyano-2-(3-phenylthiazolidin-2-ylidene) acetamido)-1,3,4-thiadiazol-2-yl)benzamide (14). Reddish brown crystals; (2.9 g, 68%); m.p. > 300 °C; IR (KBr) (υ_{max}, cm^{-1}): 3157 (NH), 3055 (CH aromatic), 2962, 2921 (CH aliphatic), 2174 (C≡N), 1673 (C=O_{amide}). ^{1}H-NMR (400 MHz, DMSO-d_6) δ_{ppm}: 3.75–3.85 (m, 4H, 2$\underline{CH_2}$), 6.72–6.77 (m, 5H, ArH), 7.55–8.05 (m, 5H, ArH), 9.21 (br s, 1H, NH, exchangeable with D_2O), 13.01 (br s, 1H, NH, exchangeable with D_2O). Anal. calcd for $C_{21}H_{16}N_6O_2S_2$ (448.52) %: C, 56.24; H, 3.60; N, 18.74; found: C, 56.29; H, 3.55; N, 18.64.

2.1.22 *N*-(6-Cyano-7-oxo-5-(phenylamino)-7*H*-[1,3,4]thiadiazolo[3,2-*a*]pyrimidin-2-yl)benzamide (15). Brown crystals; (2.7 g, 73%); m.p. > 300 °C; IR (KBr) (υ_{max}, cm^{-1}): 3418 (NH), 3060 (CH aromatic), 2923 (CH aliphatic), 2192 (C≡N), 1688 (C=O_{amide}). ^{1}H-NMR (400 MHz, DMSO-d_6) δ_{ppm}: 7.05–7.59 (m, 10H, ArH), 12.47 (br s, 1H, $\underline{NH}$Ph, exchangeable with D_2O), 13.74 (br s, 1H, NH, exchangeable with D_2O). ^{13}C-NMR (100 MHz, DMSO-d_6) δ_{ppm}: 68, 116, 117, 120, 123.32, 123.76, 126, 128, 130, 131, 134, 140, 152, 166, 169, 180. Anal. calcd for $C_{19}H_{12}N_6O_2S$ (388.41) %: C, 58.76; H, 3.11; N, 21.64; found: C, 58.65; H, 3.14; N, 21.59.

2.1.23 *N*-(5-(2-Cyano-3-(phenylamino)-3-thioxopropanamido)-1,3,4-thiadiazol-2-yl)benzamide (16). Brown crystals; (2.2 g, 54%); m.p. > 300 °C; IR (KBr) (υ_{max}, cm^{-1}): 3283, 3211 (NH), 3063 (CH aromatic), 2923 (CH aliphatic), 2205 (C≡N), 1669 (C=O_{amide}). ^{1}H-NMR (400 MHz, DMSO-d_6) δ_{ppm}: 3.5 (s, 1H, $\underline{CH}$CN), 7.46–7.67 (m, 5H, ArH), 8.12–8.13 (m, 5H, ArH), 9.24 (br s, 1H, NH, exchangeable with D_2O), 13.10 (br s, 1H, NH, exchangeable with D_2O), 13.15 (br s, 1H, $\underline{NH}$Ph, exchangeable with D_2O). Anal. calcd for $C_{19}H_{14}N_6O_2S_2$ (422.48) %: C, 54.02; H, 3.34; N, 19.89; found: C, 54.05; H, 3.36; N, 19.85.

2.1.24 *N*-(5-(2-Cyano-3,3-bis(methylthio)acrylamido)-1,3,4-thiadiazol-2-yl)benzamide (17). 1,3,4-Thiadiazole derivative **3** (2.8 g, 10 mmol) was added to a cold suspension of finely divided potassium hydroxide (0.56 g, 10 mmol) in DMF (15 mL) with stirring for 30 minutes. Carbon disulfide (2 mL) was added dropwise and then, the mixture was allowed to stand overnight. Methyl iodide (1.4 mL, 10 mmol) was added dropwise, stirred at room temperature for three hours and then, allowed to stand overnight. With stirring, the reaction mixture was placed into ice-cold dilute HCl. The separated solid was filtered, washed with water, dried, and crystallized from dioxane producing **17** as yellow crystals; (2.3 g, 60%); m.p. 250–252 °C; IR (KBr) (υ_{max}, cm^{-1}): 3160 (NH), 3002 (CH aromatic), 2932 (CH aliphatic), 2213 (C≡N), 1664 (C=O_{amide}). ^{1}H-NMR (400 MHz, DMSO-d_6) δ_{ppm}: 2.67 (s, 3H, S$\underline{CH_3}$), 2.70 (s, 3H, S$\underline{CH_3}$), 7.51–8.26 (m, 5H, ArH), 13.25 (br s, 1H, $\underline{NH}$CO, exchangeable with D_2O), 14.74 (br s, 1H, CO$\underline{NH}$, exchangeable with D_2O). ^{13}C-NMR (100 MHz, DMSO-d_6) δ_{ppm}: 20.98 (2C), 69.90, 117.06, 118.04, 121.52, 127.10, 129.60, 131.00, 132.68, 133.65, 141.38, 153.43, 167.99, 170.64. Anal. calcd for $C_{15}H_{13}N_5O_2S_3$ (391.48) %: C, 46.02; H, 3.35; N, 17.89; found: C, 46.15; H, 3.42; N, 17.93.

2.1.25 General procedure for the synthesis of compounds (18–20). A mixture of compound **17** (1.9 g, 5 mmol) and the appropriate bidentate derivatives namely, *o*-phenylenediamine (0.9 g, 5 mmol), *o*-aminophenol (0.5 g, 5 mmol), or 2,3-dihydroxypyridine (0.5 g, 5 mmol) in dioxane (10 mL) with a catalytic amount of triethylamine was refluxed for four hours. The precipitated solid was filtered off, dried, and crystallized from ethanol/dioxane [1 : 3] affording compounds **18–20**, respectively.

2.1.26 *N*-(5-(2-Cyano-2-(1,3-dihydro-2*H*-benzo[*d*]imidazole-2-ylidene)acetamido)-1,3,4-thiadiazol-2-yl)benzamide (18). Pale yellow crystals; (2.7 g, 68%); m.p. > 300 °C; IR (KBr) (υ_{max}, cm^{-1}): br. 3191 (NH), 3054 (CH aromatic), 2979 (CH aliphatic), 2171 (C≡N), br. 1688 (C=O_{amide}). ^{1}H-NMR (400 MHz, DMSO-d_6) δ_{ppm}: 7.18–7.20 (m, 2H, ArH), 7.36–7.68 (m, 5H, ArH), 8.12 (d, J = 7.52 Hz, 2H, ArH), 11.24 (br s, 1H, $\underline{NH}$CO, exchangeable with D_2O), 12.5 (br s, 2H, 2$\underline{NH}$Ph, exchangeable with D_2O), 14.52 (br s, 1H, CO$\underline{NH}$, exchangeable with D_2O). Anal. calcd for $C_{19}H_{13}N_7O_2S$ (403.42) %: C, 56.57; H, 3.25; N, 24.30; found: C, 56.47; H, 3.32; N, 24.41.

2.1.27 *N*-(5-(2-(Benzo[*d*]oxazol-2(3*H*)-ylidene)-2-cyanoacetamido)-1,3,4-thiadiazol-2-yl)benzamide (19). Pale yellow crystals; (3.4 g, 81%); m.p. 200–202 °C; IR (KBr) (υ_{max}, cm^{-1}): 3187, 3134 (NH), 3063 (CH aromatic), 2209 (C≡N), br. 1665 (C=O_{amide}), 1634 (C=N). ^{1}H-NMR (400 MHz, DMSO-d_6) δ_{ppm}: 6.73 (t, J = 7.24 Hz 1H, ArH), 6.96 (d, J = 8.72 Hz, 2H, ArH), 7.07 (d, J = 7.72 Hz, 1H, ArH), 7.21 (t, J = 8.24 Hz, 4H, ArH), 7.60 (d, J = 8.72 Hz, 1H, ArH), 10.15 (br s, 1H, $\underline{NH}$Ph, exchangeable with D_2O), 12.87 (br s, 1H, NH, exchangeable with D_2O), 14.14 (br s, 1H, NH, exchangeable with D_2O). ^{13}C-NMR (100 MHz, DMSO-d_6) δ_{ppm}: 55.62, 112.29 (2C), 114.63 (2C), 118.80, 127.50, 128.99 (2C), 129.53 (2C), 137.06 (2C), 146.06, 154.68, 155.99 (2C), 159.78, 185.65. Anal. calcd for $C_{19}H_{12}N_6O_3S$ (404.40) %: C, 56.43; H, 2.99; N, 20.78; found: C, 56.39; H, 2.85; N, 20.81.

2.1.28 *N*-(5-(2-([1,3]dioxolo[4,5-*b*]pyridin-2-ylidene)-2-cyanoacetamido)-1,3,4-thiadiazol-2-yl)benzamide (20). Brown crystals; (2.1 g, 54%); m.p. 226–228 °C; IR (KBr) (υ_{max}, cm^{-1}): 3190, 3147 (NH), 3064 (CH aromatic), 2993 (CH aliphatic), 2209 (C≡N), br. 1665 (C=O_{amide}), 1633 (C=N). ^{1}H-NMR (400 MHz, DMSO-d_6) δ_{ppm}: 7.21 (d, J = 9.12 Hz, 1H, ArH), 7.36–7.39 (m, 2H,

© 2023 The Author(s). Published by the Royal Society of Chemistry

Open Access Article. Published on 25 May 2023. Downloaded on 2/11/2026 2:26:17 AM. This article is licensed under a Creative Commons Attribution-NonCommercial 3.0 Unported Licence.

ArH), 7.59–7.63 (m, 2H, ArH), 8.01 (t, $J = 6.8$ Hz, 1H, ArH), 8.63 (d, $J = 8.3$ Hz, 2H, ArH), 11.9 (br s, 1H, NH, exchangeable with D_2O), 12.34 (br s, 1H, NH, exchangeable with D_2O). ^{13}C-NMR (100 MHz, DMSO-d_6) δ_{ppm}: 66.81, 116.04, 117.41, 120.44, 123.33, 123.69, 126.08, 128.56, 129.98, 131.66, 134.43, 158.87, 159.51, 166.93, 168.85, 169.66, 185.16, 192.83. Anal. calcd for $C_{18}H_{10}N_6O_4S$ (406.38) %: C, 53.20; H, 2.48; N, 20.68; found: C, 53.18H, 2.55; N, 20.74.

2.2. Biological evaluation

2.2.1 Antiproliferative activity. All cell lines and media were obtained from the ATCC (Virginia, USA). The cells were cultured using the media and conditions recommended by the ATCC. The cell viability was determined using MTT as described elsewhere.[12–14] Briefly, the cells were seeded at a density of 2×10^6 per well in 48-well plate. The cells were treated with the thiadiazole derivatives (0.5–100 μM) and incubated for 48 h. For comparison, untreated control cells and cells treated with doxorubicin were run under the same conditions. The data were expressed as mean ±SEM for three independent experiments. The study was approved by the Research Ethics Committee at Ain shams University and was performed in accordance with the guidelines of the National Institute of Health (NIH).

2.2.2 Cell cycle analysis. MCF-7 cells were seeded in 6-well plate (2 mL per well) overnight at 37 °C and 5% CO_2. The cells were incubated with serum-free medium for 24 hours, then cells were treated with the IC_{50} concentration of **6b** or **19** for 48 h. After incubation, cells were washed twice with ice-cold 1× PBS and collected after trypsinization. The cells were centrifuged at 500×*g* for five minutes at 4 °C. The cell pellet was resuspended in ice-cold 1× PBS and fixed with absolute ethanol and incubated at −20 °C for two hours. The fixed cells were then washed with ice-cold 1× PBS. Cell pellet was resuspended in propidium (PI)/RNase (BD Biosciences, BDB550825, NJ, USA) and incubated for 30 min at room temperature in dark, then DNA content in each phase was measured using BD FACSCanto II™ Flow Cytometer. More details could be reviewed elsewhere.[15]

2.2.3 Apoptosis assay by annexin V. MCF-7 cells were seeded in a 6-well plate (1×10^5 cells per mL) and incubated overnight at 37 °C and 5% CO_2. To a fresh medium, **DMSO**, **6b**, or **19** was added at the IC_{50} concentration and incubated for 48 hours. The cells were trypsinized, harvested, and washed twice with 1× PBS. The cells were stained with 5 μL annexin-V/FITC and 5 μL propidium iodide (Elabscience Biotechnology Inc, E-CK-A211) in the binding buffer for 15 minutes. The stained cells were analyzed by BD FACSCanto II™ flow cytometer.

2.2.4 Statistical analysis of data. The data distribution was examined by the Kolmogorov–Smirnov test. Results were expressed as mean ±SEM. The statistical analyses were performed using one-way analysis of variance followed by the Tukey-HSD test for multiple comparisons. Differences were considered significant at $p < 0.05$.

2.3. *In silico* studies

2.3.1 Docking studies. Using the MOE 2019 suite, the newly designed and synthesized compounds (**6b** and **19**) were proposed as CDK1.[16] As a result, two separate docking processes were performed for the investigated derivatives towards CDK1, with the co-crystallized inhibitor (**FB8**) serving as a reference standard.

2.3.2 Preparation of the newly designed and synthesized derivatives. As previously mentioned,[17] all of the synthesized derivatives were prepared for docking by adding partial charges and minimizing energy after being sketched using the Chem-Draw professional program and added to the MOE program window. With the extracted co-crystallized FB8 in the case of CDK1 docking process.

2.3.3 CDK-1 pockets preparation and docking. The protein data bank was used to obtain the X-ray structures of the CDK-1 proteins (PDB codes ID: 6GU7). In each case, the target proteins were 3D protonated, error corrected, and energy minimized before being docked, as previously described in detail.[18] According to each instance's default methodology, the two docking processes were carried out in accordance with the general docking protocol. For additional research, the docked poses with the most acceptable binding scores, RMSD values, and binding modes[16] were chosen.

2.3.4 Pharmacokinetic profiling. Discovery studio 2.5 was used to investigate the pharmacokinetic profile of the tested derivatives and **FB8** as previously described.

2.3.5 ADMET predictions. Using Discovery Studio 2.5, the tested candidates' ADMET descriptors-namely, absorption, distribution, metabolism, excretion, and toxicity-were assessed. According to the default protocol, the target derivatives and **FB8** were prepared and minimized.[19] After that, ADMET studies were conducted.[20]

3. Results and discussion

3.1 Chemistry

As a part of our ongoing research that aims at developing simple and efficient synthetic techniques for the synthesis of novel heterocyclic compounds with potential anticancer applications,[21–31] the present study reported the synthesis of numerous new substituted 1,3,4-thiadiazole derivatives incorporating benzene moiety. *N*-(5-Amino-1,3,4-thiadiazol-2-yl) benzamide (**2**) was synthesized as a sole product through reaction of benzoylisothiocyanate with thiosemicarbzide in dry acetonitrile and then underwent cyclization according to the previously published methodology[32–36] (Scheme 1). Treatment of compound **2** with ethyl cyanoacetate in the presence of a catalytic amount of triethylamine afforded *N*-(5-(2-cyanoacetamido)-1,3,4-thiadiazol-2-yl)benzamide (**3**) in a high yield, which was used as a key starting material (Scheme 1). The structures of compounds **2** and **3** were deduced from their elemental and spectral analyses.

The nucleophilic reactivity of the intermediate **3** towards various carbon electrophiles has been investigated. Refluxing compound **3** with salicylaldehyde in an ethanolic solution containing a catalytic amount of piperidine yielded 2-iminocoumarin derivative **4** (Scheme 2). The presence of absorption bands for –NH groups at 3409 and 3158 cm^{-1} along with the absence of absorption band for the nitrile group confirmed the assigned

Open Access Article. Published on 25 May 2023. Downloaded on 2/11/2026 2:26:17 AM.
This article is licensed under a Creative Commons Attribution-NonCommercial 3.0 Unported Licence.

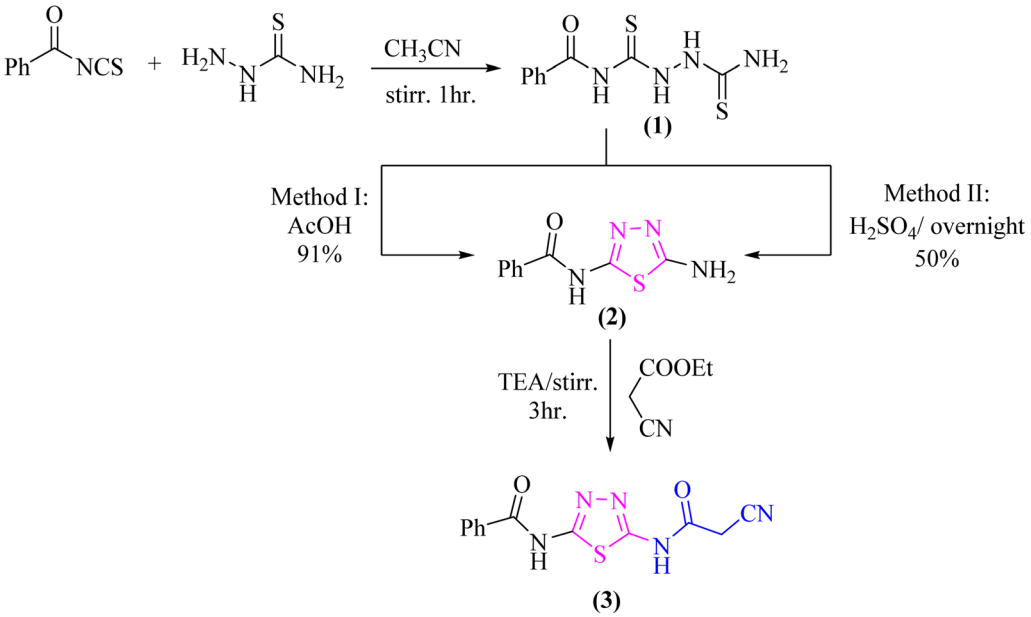

Scheme 1 Synthesis of 1,3,4-thiadiazole derivative **3**.

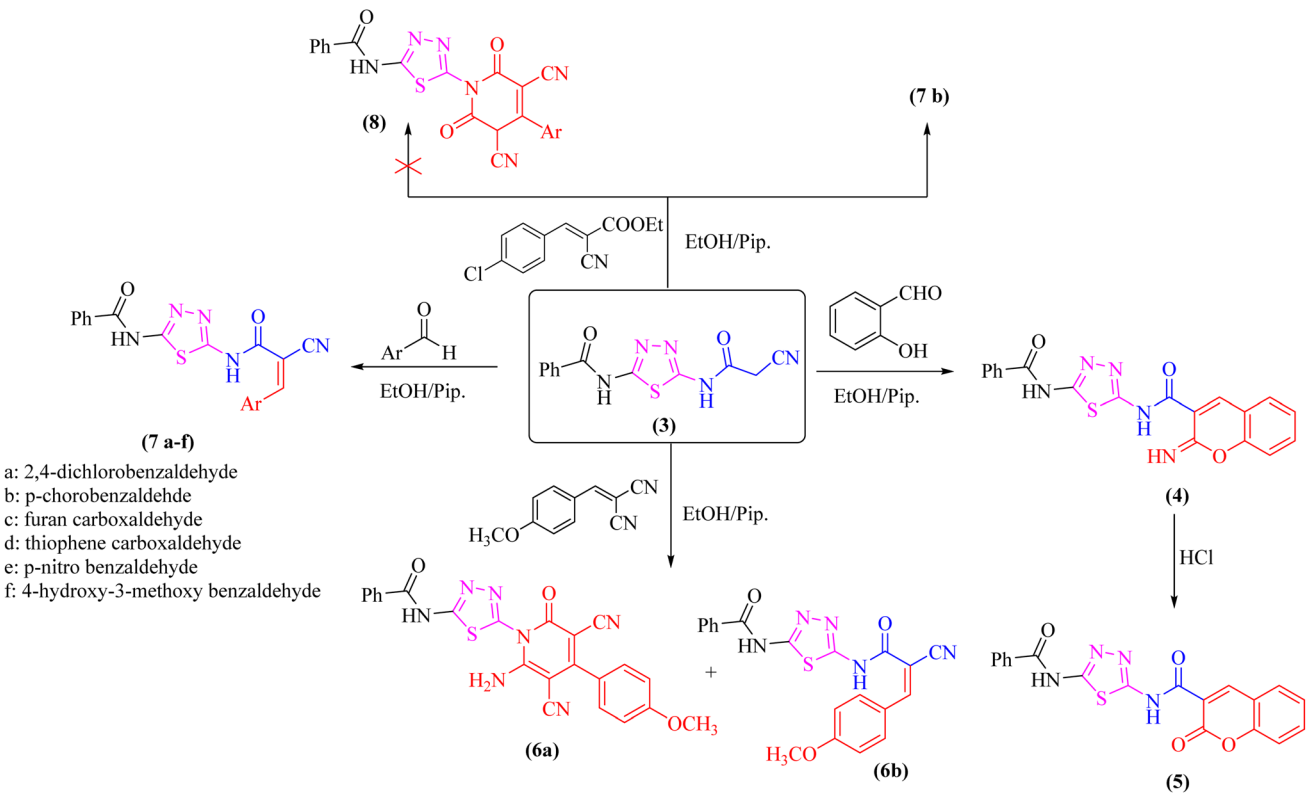

Scheme 2 Reaction of the β-ketonitrile **3** with some aromatic aldehydes and arylidene derivatives.

structure **4**. In addition, acidification of the filtrate gave the expected coumarin derivative **5** (Scheme 2). Ample evidence for the assigned structure **5** was forthcoming from the correct elemental analysis and spectral data. The presence of a high frequency C=O stretching at 1713 cm^{-1} was attributed to the coumarin oxo-group in the IR spectrum as well as the absence of NH proton of imino group at 11.76 ppm in the ^{1}H-NMR spectrum of compound **5** agrees well with the proposed structure.

Subjecting compound **3** to react with 2-(4-methoxybenzylidene)malononitrile gave a grey crystalline product

© 2023 The Author(s). Published by the Royal Society of Chemistry

Open Access Article. Published on 25 May 2023. Downloaded on 2/11/2026 2:26:17 AM.
This article is licensed under a Creative Commons Attribution-NonCommercial 3.0 Unported Licence.

upon reflux which was identified as 2-oxopyridine thiadiazole derivative **6a** (major product, Scheme 2), while acidification of the reaction filtrate with cold dilute HCl furnished an orange precipitate that was detected as the arylidene derivative **6b** (minor product). Furthermore, the Knoevenagel condensation of 1,3,4-thiadiazole derivative **3** with aromatic aldehydes namely; 2,4-dichlorobenzaldehde, *p*-chlorobenzaldehyde, furan-2-carbaldehyde, thiophene-2-carbaldehyde, *p*-nitro benzaldehyde, or 4-hydroxy-3-methoxy benzaldehyde for three hours in refluxing ethanol containing a catalytic amount of piperidine afforded the corresponding arylidene derivatives **7a–f**, respectively (Scheme 2). Moreover, the reaction of compound **3** with ethyl 3-(4-chlorophenyl)-2-cyanoacrylate under the same reaction conditions afforded the arylidene derivative **7b** rather than 2-oxopyridin derivative **8**.

The proclivity of thiadiazole derivative **3** towards β-diketones was also investigated in this study. Thus, 2-pyridone derivatives **9** and **10** were obtained from the reaction of **3** with acetyl acetone and benzoyl acetone, respectively in ethanolic solution containing catalytic amount of fused sodium acetate (Scheme 3). ^{1}H-NMR spectrum of compound **9** showed signals at 3.96 and 3.99 ppm which were attributed to protons of CH_3 group, as well as the absence of a singlet signal for protons of CH_2CN group which confirmed the proposed structure **9**. Furthermore, the ^{13}C-NMR spectrum revealed the presence of two methyl groups at δ 21.01 and 21.12 ppm (Scheme 3).

At room temperature, the active methylene moiety in the cyanoacetamide derivative **3** readily adds to one carbon donor such as phenyl isothiocyanate in DMF-containing potassium hydroxide forming a non-isolable intermediate potassium thiocarbamate salt (**A**), which *in situ* reacted with ethyl chloroacetate, chloroacetyl chloride, diethylmalonate, 1,2-dibromo ethane, methyliodide, or hydrochloric acid giving the corresponding ethyl thioacetate, 1,3-thiazolone, 4,6-dioxo-1,3-thiazinan, 1,3-thiazole, thiadiazolo[3,2-*a*]pyrimidin, and thioxopropanamide derivatives **11–16**, respectively (Scheme 4). The structures of derivatives **11–16** were clarified using elemental analysis and spectral data (*c.f.* experimental). For instance, the appearance of strong absorption bands in the IR spectrum at 2195 and 1734 cm^{-1} for C≡N and C=O$_{ester}$ groups, respectively was completely consistent with the suggested structure **11** and ruled out the cyclized compound **12**.

Likewise, addition of 1,3,4-thiadiazole derivative **3** to carbon disulfide in DMF-containing potassium hydroxide at room temperature gave the non-isolable dipotassium dithiocarbazate salt (**B**), which *in situ* reacted with methyl iodide affording the ketene *S*,*S*-dithioacetal **17** (Scheme 5). The elemental analysis and spectral data were used to determine the structure of compound **17**.

Further, the reactivity of **17** towards some nitrogen and oxygen nucleophiles was investigated. Thus, compound **17** reacted under reflux with bidentate nucleophiles such as *o*-phenylenediamine, *o*-aminophenol, or 2,3-dihydroxy pyridine giving the corresponding benzimidazole derivative **18**, benzoxazole derivative **19**, and dioxolo[4,5-*b*]pyridine derivative **20**, respectively (Scheme 5). The structures of compounds **18–20** were consistent with the ^{1}H-NMR and ^{13}C-NMR spectra which revealed the absence of two SCH_3 groups.

3.2 Biological evaluation

3.2.1 Antiproliferative activity. According to the National Cancer Institute (NCI) criteria, only novel moieties with antiproliferative activity at 10 μM or less against cancer cell lines are considered for further studies.[37] Based on this criterion, only derivatives **4**, **6b**, **7a**, **7d**, and **19** are to be considered (Table 1). However, derivatives **4** and **7d** were only effective against the breast cells and with very low selectivity. Although derivative **7a** was effective against all cell lines investigated, it has a low selectivity index (SI = 1.5). In other words, derivatives **4**, **7a**, and **7d** were as toxic to the cancer cells as to the normal fibroblasts, and therefore, these derivatives were excluded from further investigations (Table 1). Derivatives **6b** and **19** with IC_{50} at less than 10 μM against the breast, colon, and prostate cell lines and with high selectivity (SI = ~5 and 6 folds, respectively), were

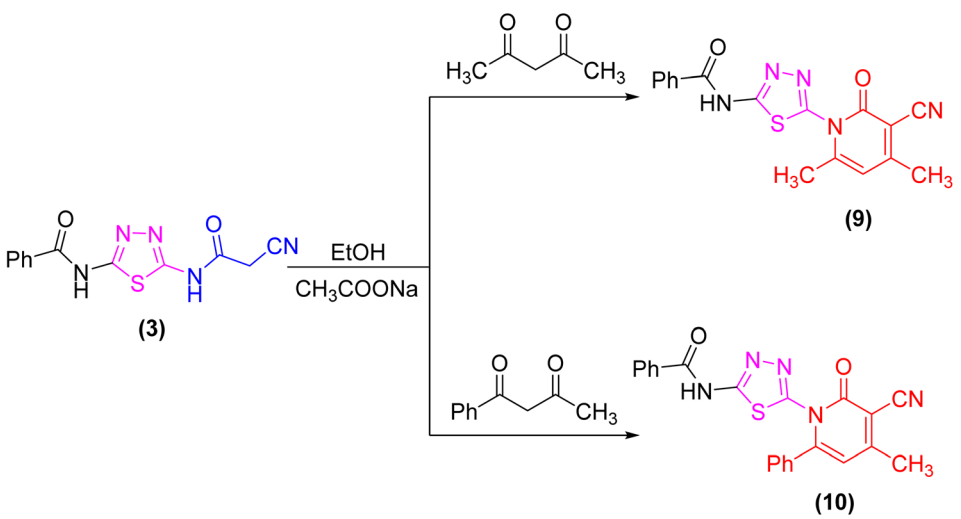

Scheme 3 Synthesis of some new 2-pyridone derivatives (**9** and **10**) from the cyanoacetamide **3**.

Open Access Article. Published on 25 May 2023. Downloaded on 2/11/2026 2:26:17 AM.
This article is licensed under a Creative Commons Attribution-NonCommercial 3.0 Unported Licence.

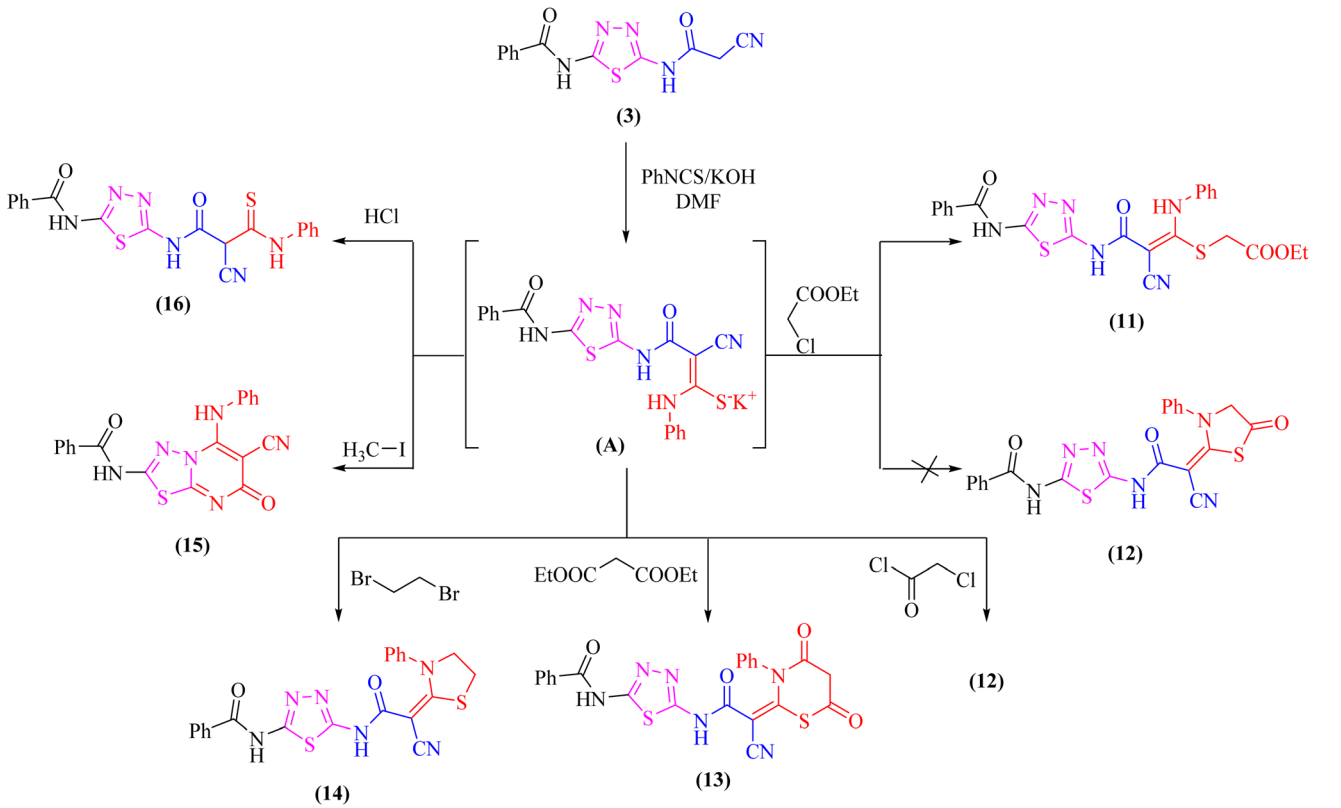

Scheme 4 Reaction of potassium thiocarbamate (A) with some electrophiles.

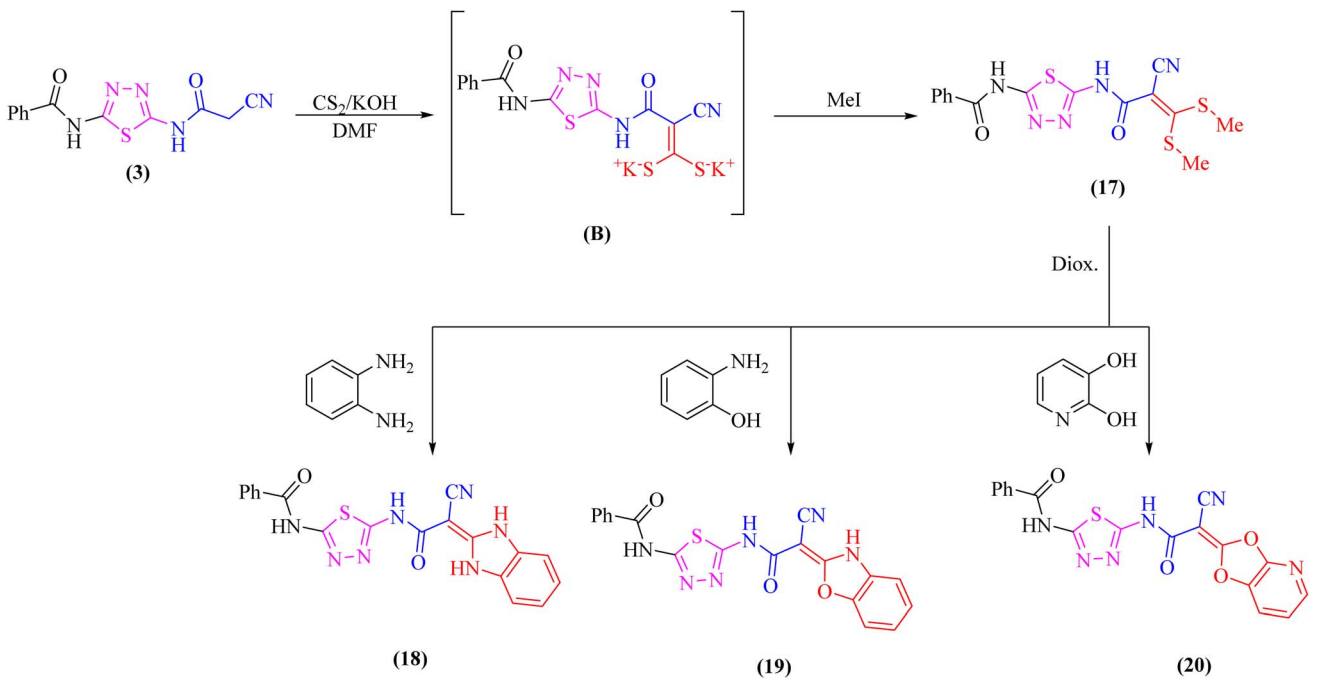

Scheme 5 Treatment of the ketene *S*,*S*-dithioacetal **17** with some bidentate nucleophiles.

selected for further studies. It is noteworthy that other than **7a**, no other derivative exhibited a significant antiproliferative activity against the liver HepG2 cells. It is also noteworthy that 18 compounds out of 24 were toxic (not selective) to the normal fibroblasts. Doxorubicin had antiproliferative activity against all cell lines investigated with no selectivity (SI = 1.2). The breast

© 2023 The Author(s). Published by the Royal Society of Chemistry

Open Access Article. Published on 25 May 2023. Downloaded on 2/11/2026 2:26:17 AM. This article is licensed under a Creative Commons Attribution-NonCommercial 3.0 Unported Licence.

Table 1 The antiproliferative activity (IC_{50} in μM) of the new thiadiazole derivatives against human breast (MCF-7), colon (HCT-116), prostate (PC-3), and liver (HepG2) cell lines, and normal fibroblasts (WI-38) and their selectivity index (SI)[a]

Cpds	MCF-7	HCT-116	PC-3	HepG2	WI-38	SI[c]
DOX	4.17 ± 0.2[b]	5.23 ± 0.3[b]	8.87 ± 0.6[b]	4.50 ± 0.2[b]	6.72 ± 0.5[b]	1.2
2	12.36 ± 3.0	15.26 ± 2.8	30.01 ± 3.1	14.11 ± 1.5	17.56 ± 4.1	1.0
3	23.81 ± 1.9	25.72 ± 1.9	39.23 ± 2.8	31.26 ± 5.1	37.41 ± 2.5	1.2
4	8.25 ± 3.5[b]	15.84 ± 3.2	20.97 ± 3.3	48.51 ± 2.9	29.35 ± 2.2	1.3
5	64.12 ± 3.8	47.22 ± 3.5	66.53 ± 3.9	63.93 ± 8.9	91.23 ± 4.6	1.5
6a	41.57 ± 2.7	29.19 ± 2.3	35.76 ± 2.6	54.62 ± 6.8	18.64 ± 1.4	0.5
6b	9.48 ± 0.8[b]	8.15 ± 0.7[b]	7.41 ± 0.6[b]	15.88 ± 1.3	50.39 ± 0.9	4.9
7a	5.51 ± 0.4[b]	3.97 ± 0.2[b]	9.10 ± 0.8[b]	6.34 ± 0.9[b]	9.18 ± 3.6[b]	1.5
7b	17.73 ± 0.6	16.18 ± 0.4	21.86 ± 1.1	14.68 ± 2.1	42.06 ± 2.7	2.4
7c	28.13 ± 3.5	52.63 ± 3.7	13.30 ± 3.6	16.34 ± 1.8	22.57 ± 3.0	0.8
7d	8.02 ± 1.4[b]	34.14 ± 2.6	11.12 ± 4.7	66.10 ± 3.5	12.28 ± 1.2	0.4
7e	45.11 ± 4.0	51.39 ± 4.1	75.22 ± 4.7	56.33 ± 7.8	23.39 ± 3.6	0.4
7f	13.59 ± 1.1	10.92 ± 0.9	18.35 ± 1.5	21.26 ± 3.7	14.54 ± 0.3	0.9
9	14.13 ± 1.2	12.78 ± 1.1	15.38 ± 1.3	39.07 ± 2.7	50.39 ± 0.9	2.5
10	72.41 ± 4.1	68.01 ± 3.9	86.47 ± 4.8	19.40 ± 1.5	>100	1.7
11	69.70 ± 3.9	63.12 ± 3.8	71.94 ± 4.0	52.87 ± 4.6	22.65 ± 3.8	0.4
12	84.81 ± 4.4	91.27 ± 4.6	>100	69.54 ± 6.5	>100	1.2
13	37.95 ± 3.2	46.14 ± 3.7	73.56 ± 4.3	45.21 ± 6.3	23.58 ± 3.2	0.5
14	36.23 ± 2.4	40.18 ± 3.1	92.28 ± 3.2	>100	53.75 ± 3.4	0.8
15	12.74 ± 2.1	17.03 ± 1.4	10.49 ± 1.9	16.84 ± 1.7	19.38 ± 1.5	1.4
16	19.58 ± 1.6	21.62 ± 1.7	28.80 ± 2.3	14.68 ± 2.3	85.91 ± 1.9	4.1
17	15.10 ± 1.3	14.67 ± 0.9	12.17 ± 0.8	12.47 ± 1.0	81.20 ± 4.1	6.0
18	84.65 ± 4.6	56.85 ± 3.6	81.82 ± 4.5	47.33 ± 8.2	>100	1.5
19	7.70 ± 0.5[b]	5.98 ± 0.3[b]	6.35 ± 0.5[b]	19.40 ± 1.5	60.28 ± 3.7	6.1
20	36.78 ± 2.7	18.32 ± 1.7	31.39 ± 2.2	29.64 ± 3.1	42.74 ± 2.7	1.5

[a] The IC_{50} was calculated from a dose–response curve. Doxorubicin (Dox) was used as a positive control. The data are expressed as mean ±SEM from three independent experiments. [b] Significant (less than 10 μM) antiproliferative activity as compared to the untreated cells. [c] SI: selectivity index = WI-38 IC_{50}/IC_{50} against cancer cells.

cells (MCF-7) were the most responsive to the thiadiazole derivatives. Therefore, these cells were selected for further investigations on compounds **6b** and **19**.

3.2.2 Cell cycle and apoptosis analysis. In the cell cycle analysis assay, the treated cells are stained with propidium iodide (DNA binding stain) and analyzed by flow cytometry. Treatment of MCF7 cells with **19** led to G2/M arrest with 23.3% of cells arrested at this stage compared to 4.6% in the cells treated with **DMSO** (Fig. 2). The arrested cells usually undergo apoptosis. Compound **6b** increased the sub-G1 percent of cells from 7.4% in the **DMSO**-treated cells to 53.6%. The sub-G1 population is characterized by low DNA level, and it is usually comprised of cell fragments, often because of apoptosis or sometimes necrosis. Since the sub-G1 peak appears very close to the G0/G1 peak, we believe it is mainly due to necrosis rather than to apoptosis. To exclude the contribution of any mechanical stress to the cells from excessive pipetting, vortex, or harsh centrifugation that usually results in elevation of the sub-G1 cell population, the experiment was repeated thrice with much care and restricted gating strategy.

The arrest of cells at the G2/M indicates a severe DNA damage that is beyond repair.[38] The crucial event in cell-cycle progression through the G2/M checkpoint is the upregulation of expression of Chk2 protein and increase in the phosphorylation of Chk2 and CDC25C, leading to inhibition of the formation CDK1/cyclin B complex and cell cycle arrest at the G2/M phase.[39,40] Many proteins such as p53, p21, and p38/MAPK could contribute to the arrest at the G2/M phase.[41] p53 induces the transcription of p21 which inhibits CDK resulting in the arrest of cells at the G2/M.[42,43] In the current study, we have not investigated these different pathways.

We have also measured apoptosis by annexin V-PI assay. The level of apoptotic cells either in the early stage (lower-right quadrant, LR) or late apoptotic stage (upper-right quadrant, UR), in addition to the necrotic cells in the upper left (UL) quadrant were all quantified by flow cytometry (Fig. 3). It is evident that compound **6b** did not induce apoptosis and increased the necrotic cells by 12.5% compared to 0.1% when the cells were treated with **DMSO**. This confirms the data we have obtained from the cell cycle analysis. As expected, compound **19** significantly increased the early apoptosis to 15% and increased the necrotic cells to 15% (Fig. 3). Compound **19** evidently arrested the cells at the G2/M forcing them to apoptosis possibly through induction of p53 and different caspases.[44–46] Derivatives **6b** and **19** induced necrosis in addition to the apoptosis caused by derivative **19**. Although the importance of necrosis in the cancer therapy is not as fully understood as apoptosis, recent studies suggest that necrosis or necroptosis have potential applications as anticancer target.[47,48]

3.3. *In silico* studies

3.3.1 Molecular docking study. First, two validation procedures were completed to verify the MOE program's

Open Access Article. Published on 25 May 2023. Downloaded on 2/11/2026 2:26:17 AM.
This article is licensed under a Creative Commons Attribution-NonCommercial 3.0 Unported Licence.

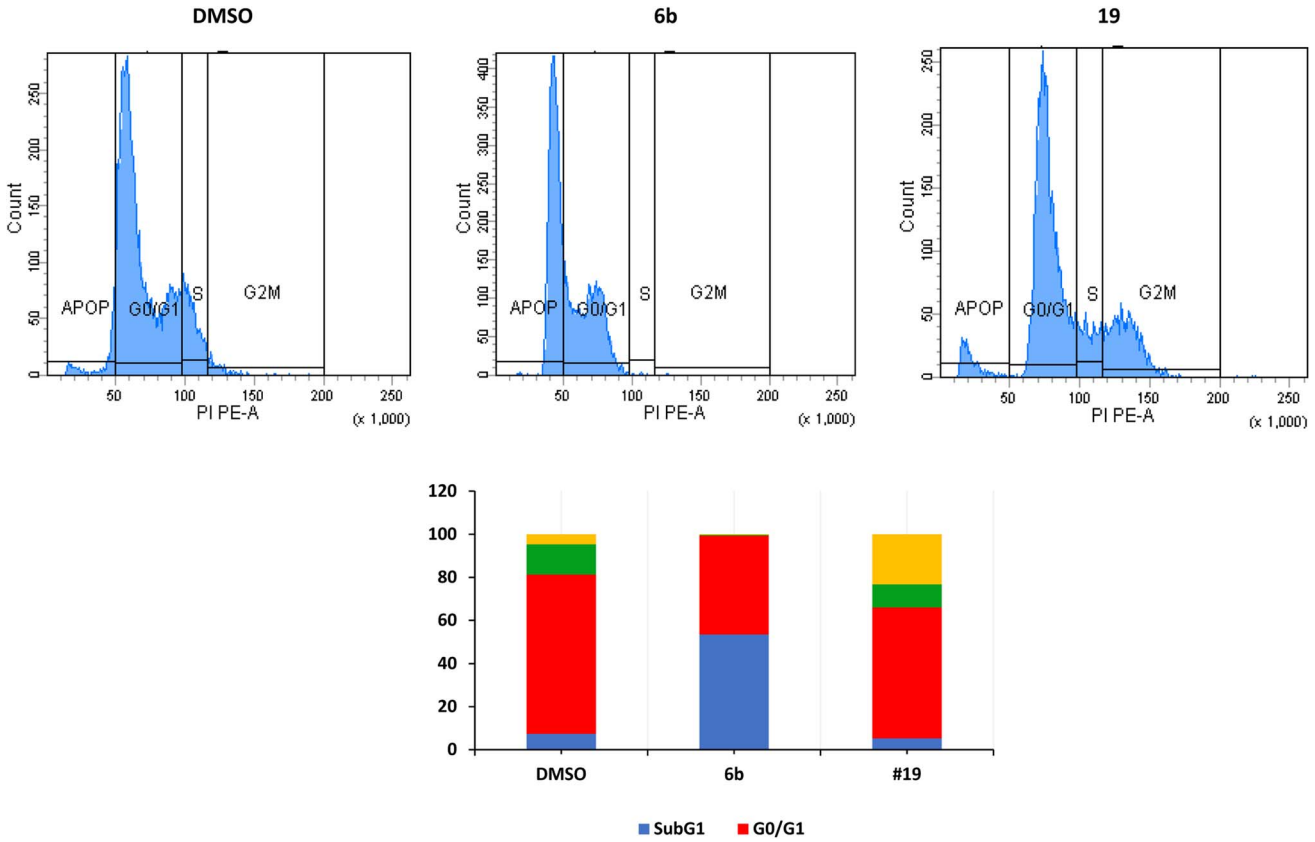

Fig. 2 Cell cycle analysis of MCF7 after treatment with derivatives **6b** and **19**. Data are expressed as means ±SEM ($n = 3$). The top panel represents one sample, and the bottom figure represents the average of 3 independent experiments expressed as percentage of cells in every stage.

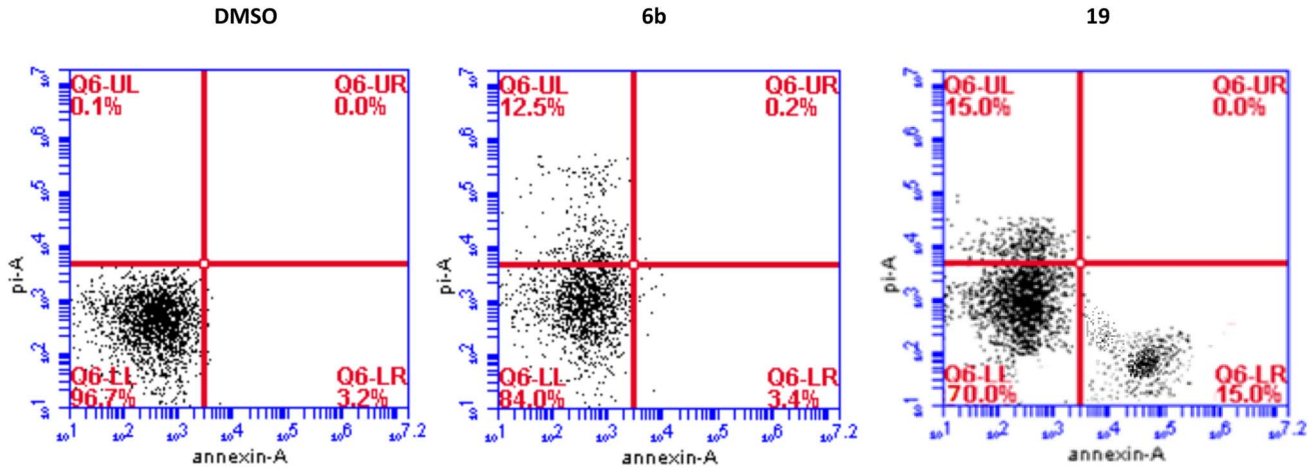

Fig. 3 Detection of apoptosis by derivatives **6b** and **19** in MCF7 cells by flow cytometry.

reliability in producing accurate docking results. This was proven by redocking the co-crystallized inhibitor of the CDK-1.[49] The successful execution of the docking protocol was guaranteed by the low values of RMSD = 1.043 Å that were obtained between the native and redocked poses of the co-crystallized inhibitor.[50]

It was shown that **FB8**, a native co-crystallized inhibitor of the CDK-1, forms four H-bonds with the amino acids Glu81, Leu83, Leu83 and Lys89, one ionic bond with Asp146, and one pi-bond with Phe80.[49] More thorough research and comparisons with the docked **FB8** of the CDK-1 binding pocket was conducted on the two most promising biologically active newly synthesized thiadiazol derivatives (**6b** and **19**). After looking at

© 2023 The Author(s). Published by the Royal Society of Chemistry

Open Access Article. Published on 25 May 2023. Downloaded on 2/11/2026 2:26:17 AM.
This article is licensed under a Creative Commons Attribution-NonCommercial 3.0 Unported Licence.

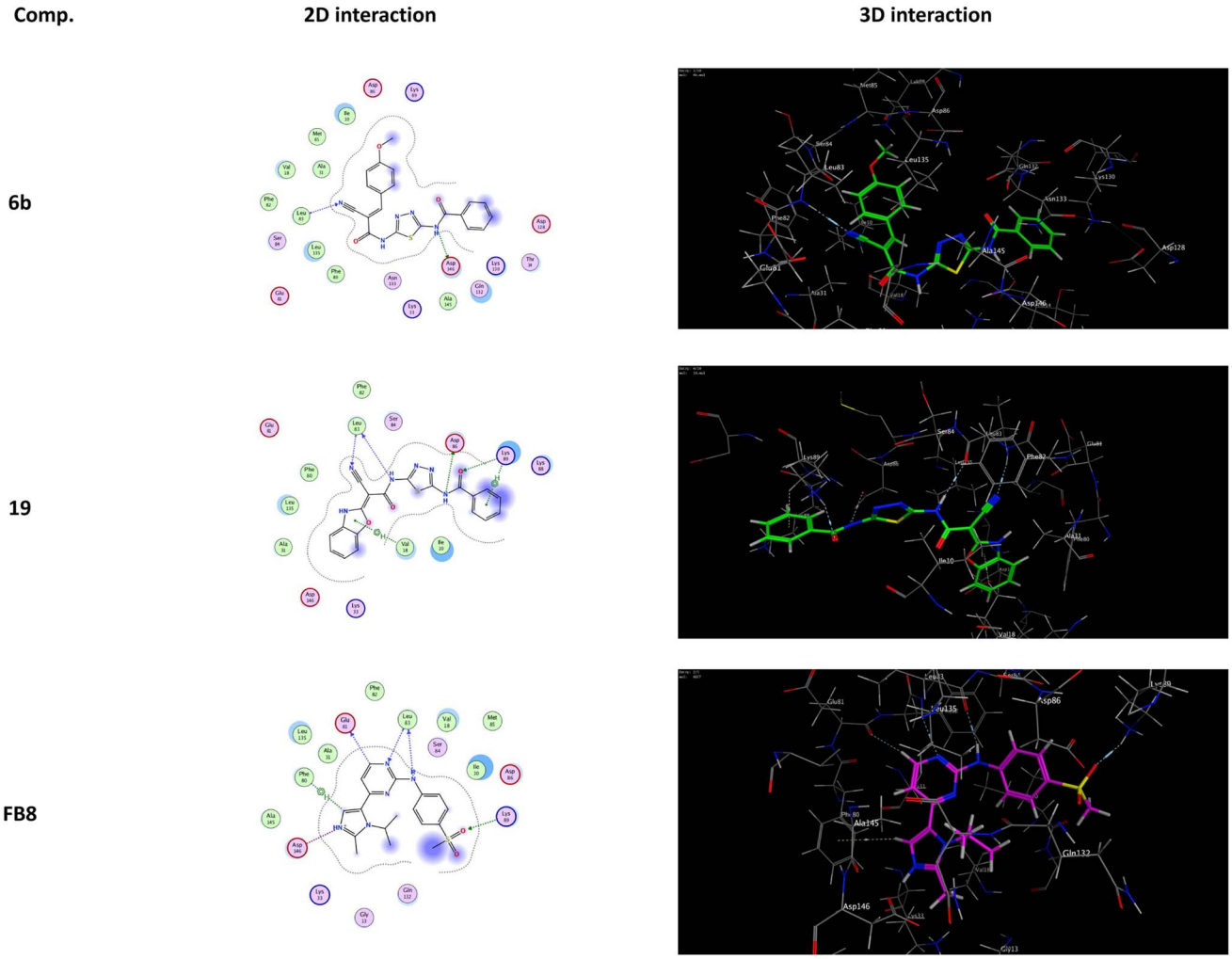

Fig. 4 The interactions of the most promising derivatives (**6b** and **19**) at CDK-1 binding pocket, alongside the docked co-crystallized inhibitor (**FB8**), are depicted in 2D and 3D interactions. H-bonds (dashed blue lines), ionic bond (red dashed lines) and H–pi bonds (green dashed lines).

the binding modes of the aforementioned compounds (Fig. 4), we concluded that:

(a) Compound **6b** formed a H-bond donor with the Asp146 amino acids at 2.97 Å and a H-bond acceptor with the Leu83 amino acid at 3.17 Å when positioned inside the largest binding pocket of the CDK-1 ($S = -7.220$ kcal mol^{-1} and RMSD = 1.713). It is not a good inhibitor of the enzyme.

(b) Compound **19** formed two H-bonds donor with Leu83 and Asp86 amino acids at 3.53 and 2.93 Å, respectively. Furthermore, it formed two H-bonds acceptor with Lys89 and Leu83 amino acid at 3.03 and 3.18 Å, respectively, as well as two pi–H bonds with Val18 and Lys89 amino acids at 3.78 and 3.66 Å, respectively inside the binding site of the CDK-1 ($S = -6.671$ kcal mol^{-1} and RMSD = 1.067). Therefore, compound **19** is a good CDK1 inhibitor candidate.

(c) Finally, it was shown that the docked co-crystallized inhibitor of the CDK-1 (FB8, $S = -6.787$ kcal mol^{-1} and RMSD = 1.124) formed two H-bonds donor with Glu81 and Leu83 amino acid at 3.39 and 2.99 Å, respectively. Furthermore, it formed two H-bonds acceptor with Leu83 and Lys89 amino acid at 3.42 and 3.13 Å, respectively. Also, formed one pi–H bond with Phe80 amino acids at 4.42 Å. In addition to one ionic bond with Asp146 amino acid at 4.42 Å.

3.3.2 Pharmacokinetics profiling study. In the current study, **FB8** was used as a reference compound to assess the pharmacokinetics and physicochemical properties of all the designed compounds *in silico*.[51,52] According to Lipinski, a molecule is predicted to be absorbed more effectively if it complies with at least three of the following four principles: (i) molecular weight <500; (ii) H-bond donors [HBD] (OH, NH, and SH) ≤5; (iii) H-bond acceptors [HBA] (N, O, and S atoms) ≤10; (iv) log P < 5. More than one of these requirements must be met for a compound to have a high level of bioavailability. Additionally, it was found that the number of rotatable bonds and the reduction in molecular flexibility were important indicators of excellent oral bioavailability.[53] For substances with ten or fewer rotatable bonds and a molecular polar surface area of 140 Å or less, oral bioavailability is likely to be high.[54]

Except for compound **11**, which violates more than one of the Lipinski's rule of five, all tested, and reference compound

© 2023 The Author(s). Published by the Royal Society of Chemistry

Open Access Article. Published on 25 May 2023. Downloaded on 2/11/2026 2:26:17 AM. This article is licensed under a Creative Commons Attribution-NonCommercial 3.0 Unported Licence.

Table 2 Physicochemical characteristics of the new thiadiazole derivatives and the reference compound

	Lipinski's rule of five					Verber's rule	
Comp	log *P*	Mol. wt	HBD	HBA	Violation of Lipinski's rule	Number of rotatable bonds	TPSA
2	1.13	220.25	2	3	0	3	109.14
3	0.95	287.30	2	5	0	6	136.01
4	2.66	391.40	3	6	0	6	149.21
5	2.57	392.39	2	6	0	6	142.43
6a	2.42	469.48	2	7	0	6	187.95
6b	2.58	405.43	2	6	0	8	145.24
7a	3.59	444.29	2	5	0	7	136.01
7b	3.07	409.85	2	5	0	7	136.01
7c	1.86	365.37	2	6	0	7	149.15
7d	2.53	381.43	2	5	0	7	164.25
7e	1.91	420.40	2	7	0	8	181.83
7f	2.25	421.43	3	7	0	8	165.47
9	2.39	351.38	1	5	0	4	128.91
10	3.30	413.45	1	5	0	5	128.91
11	3.00	508.57	3	7	2	13	199.64
12	2.32	462.50	2	6	0	7	181.62
13	1.88	490.51	2	7	0	7	198.69
14	2.62	448.52	2	5	0	7	164.55
15	2.57	388.40	2	5	0	5	140.42
16	2.45	422.48	3	5	0	9	180.13
17	2.16	391.49	2	5	0	8	186.61
18	1.78	403.42	4	5	0	6	167.59
19	2.11	404.40	3	6	0	6	164.94
20	1.60	406.37	2	8	0	6	167.36
FB8	2.51	371.46	1	5	0	5	98.15

(**FB8**) listed in Table 2 displayed drug-like molecular (DLM) nature, according to the study. Only one of Lipinski's rule of five was violated and only by compound **11**. All other investigated molecules had log *P*, molecular weight, number of H-bond donors, and number of H-bond acceptors less than 5, 500, 5, and 10, respectively. Except for compound **11**, which showed 13 rotatable bonds, all the examined molecules' topology polar surface areas (TPSA) and numbers of ratable bonds fall within the acceptable ranges of less than 10 and 140 Å, respectively.

3.3.3 ADMET analysis. All the compounds examined were subjected to ADMET analyses using Discovery Studio 2.5, with the reference compound **FB8**. Many descriptors were used in ADMET evaluations, including hepatotoxicity, intestinal absorption, aqueous solubility, plasma protein binding, and molecular blood–brain barrier (BBB) penetration,[55] Table 3.

The results showed that BBB penetration levels varied from none (derivatives **2**, **4**, **9**, **11**, **18**, and **20**, in addition to **FB8**) to very high (derivatives **5**, **7a–f**, **13**, and **14**). Derivatives **3**, **6a**, **6b**, **10**, **12**, **15–17**, and **19** showed low penetration ability to the BBB. Most important that derivatives **6b** and **19** are safe to the CNS.

Clinical trials for a number of pharmaceutical candidates have been documented as being unsuccessful because of absorption issues.[56] Intestinal absorption is the proportion of a drug that is taken up by the intestinal mucosa. A drug is well-absorbed if at least 90% of it is absorbed into the bloodstream.[57] All the tested compounds, except for **5**, **7a–f**, **13** and **14**, which showed moderate to poor levels of absorption, have good absorption properties, according to the findings of these studies. All the novel compounds as well as the reference

Table 3 Predicted ADMET descriptions for the thiadiazoles and **FB8**

Comp	BBB level[a]	Absorption level[b]	Hepatotoxicity probability[c]	PPB[d]
2	0	0	0.857	0
3	1	0	0.901	0
4	0	0	0.834	2
5	4	2	0.518	2
6a	1	0	0.909	2
6b	1	0	0.878	2
7a	4	1	0.89	2
7b	4	1	0.530	2
7c	4	1	0.887	2
7d	4	2	0.87	2
7e	4	2	0.516	2
7f	4	2	0.894	2
9	0	0	0.86	2
10	1	0	0.974	1
11	0	0	0.907	2
12	2	0	0.859	2
13	4	2	0.905	2
14	4	2	0.955	2
15	1	0	0.905	2
16	1	0	0.865	2
17	1	0	0.794	2
18	0	0	0.92	2
19	1	0	0.973	1
20	0	0	0.912	2
FB8	0	2	0.517	1

[a] BBB level, blood–brain barrier level, 0 = very high, 1 = high, 2 = medium, 3 = low, 4 = very low. [b] Absorption level, 0 = good, 1 = moderate, 2 = poor, 3 = very poor. [c] Hepatotoxicity probability, value > 0.5 means toxic, value < 0.5 means non-toxic. [d] PPB, plasma protein binding, 0 means less than 90%, 1 means more than 90%, 2 means more than 95%.

© 2023 The Author(s). Published by the Royal Society of Chemistry

Open Access Article. Published on 25 May 2023. Downloaded on 2/11/2026 2:26:17 AM.
This article is licensed under a Creative Commons Attribution-NonCommercial 3.0 Unported Licence.

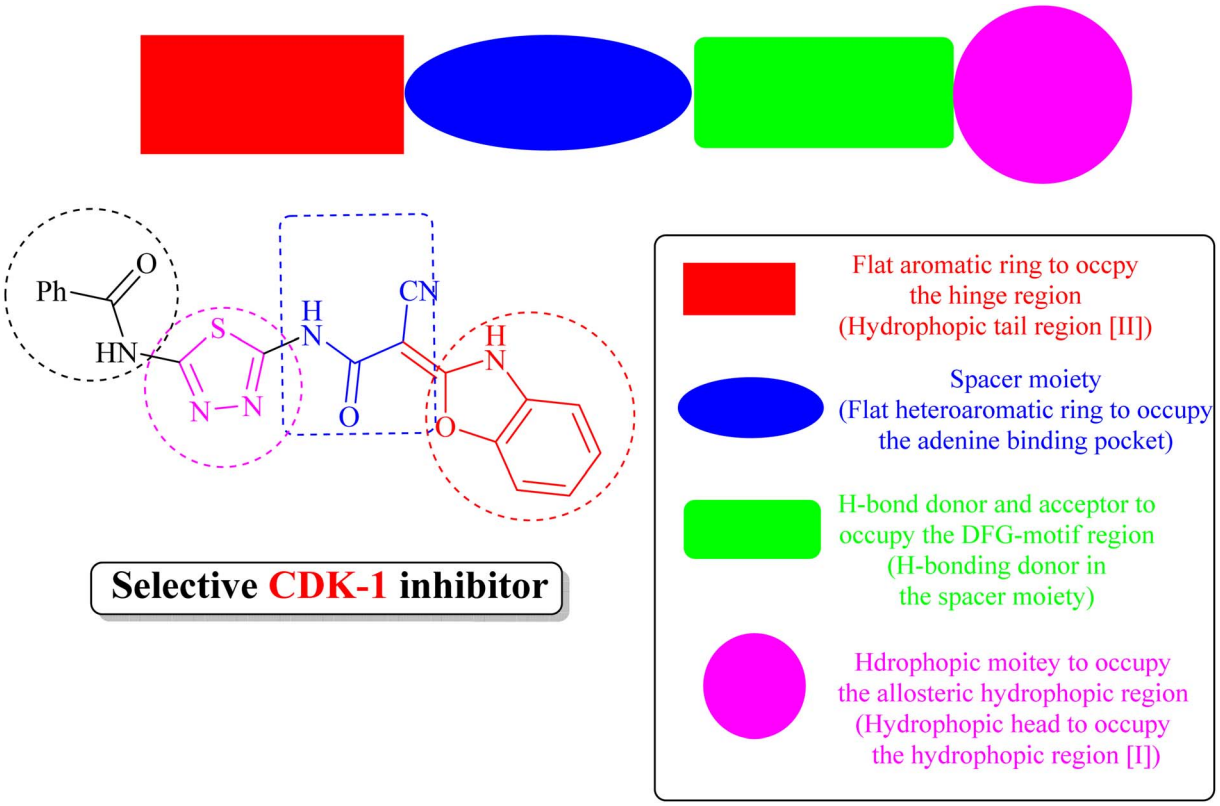

Fig. 5 Derivative **19** as a potential inhibitor of CDK1.

compound could have potential hepatotoxic effects according to predictions. All tested members and reference compound can bind plasma protein greater than 90% (highly bound), except for compounds **2** and **3**, which showed plasma protein binding less than 90%.

3.4 Structure activity relationship (SAR) study

The SAR of the newly synthesized derivatives of the two series of thiadiazole and benzoxazole-based yields very promising results.

(i) Concerning the antiproliferative activity of thiadiazole-based derivatives, compound **6b** was found to be superior to compound **7a** and then compound **7d** on the four cell lines studied. This indicates that the 4-CH_3 substituent on the side phenyl moiety is superior to the 2,4-diCl substituent, which is also superior to the thiophene moiety.

(ii) In contrast, we can conclude about the benzoxazole-based candidate compound **19** with benzo[*d*]oxazole ring together with the thiadiazole moiety achieved the best antiproliferative actions. The cyanoacetamido moiety in position-2 of the benzoxazole ring and benzamide side chain, demonstrated strong anti-proliferative effects on all four cancer cell lines.

(iii) Derivative **19** shares some of the common characteristics of the known CDK1 inhibitors (Fig. 5). These include a hydrophobic head to occupy the hydrophobic region I, an H-bond donor in the spacer moiety, a flat heteroaromatic ring to occupy the ATP-binding pocket, and a hydrophobic tail to occupy the hydrophobic region I. In addition, derivative **19** has various H-bond donor and/or acceptor moieties such as cyanoacetamide. The presence of a linker (thiourea or cyanoacetamide) or rigidified to heteroaromatic ring facilitates the occupation to the hydrophobic region of the enzyme. A substituted phenyl ring and heteroaromatic ring with various electron-donating or withdrawing groups added to the aforementioned core probably improved the inhibiting potential of derivative **19**.

4. Conclusion

In this study, a group of 24 annulated 1,3,4-thiadiazole compounds were synthesized and investigated as anticancer agents. Only five derivatives had a significant antiproliferative activity against a panel of four cancer cell lines. However, three of these were not selective and caused toxicity to the normal cells. Two derivatives **6b** and **19** were effective and selective. Compound **19** arrested the MCF-7 cells at the G2/M phase probably through inhibition of CDK1 and elicited apoptosis in these cells confirmed by the annexin V-PI assay. Compound **6b** acted through a different pathway and significantly increased the sub-G1 percent of cells probably through induction of necrosis. Molecular docking showed that compound **19** is a potential CDK1 inhibitor candidate. Derivatives **6b** and **19** did not violate Lipinski's rule of five and therefore, they are considered hits for further drug discovery research. *In silico* studies showed that these derivatives also have a low blood–brain barrier penetration capability and high intestinal

Open Access Article. Published on 25 May 2023. Downloaded on 2/11/2026 2:26:17 AM. This article is licensed under a Creative Commons Attribution-NonCommercial 3.0 Unported Licence.

absorption. Taken together, derivatives **6b** and **19** could serve as potential anticancer agents and merit further investigations.

Author contributions

Data curation: PSF and WME. Formal analysis: PSF and WME. Investigation: MHH, PSF, and WME. Writing – original draft: MHH, PSF, and WME. Conceptualization: MHH, MMH, WME. Supervision: MMH. Resources: AAE, AIH, WME. Software: PSF. Methodology: MHH, PSF, and WME. Validation: MHH, WME. Writing – review & editing: PSF, and WME. All authors read and approved the final version of the manuscript.

Conflicts of interest

Authors declare that they have no conflict of interest.

References

1 A. Kumar, A. K. Singh, H. Singh, V. Vijayan, D. Kumar, J. Naik, et al., *Pharmaceuticals*, 2023, **16**(2), 1–68.
2 S. Pearce, *Drug Discvery*, 2017, **67**, 66–70.
3 J. Bostrom, A. Hogner, A. Llinas, E. Wellner and A. T. Plowright, *J. Med. Chem.*, 2012, **55**, 1817–1830.
4 C. D. Monte, S. Carradori, D. Secci, M. D'Ascenzio, P. Guglielmi, A. Mollica, S. Morrone, S. Scarpa, A. M. Aglianò, S. Giantulli and I. Silvestri, *Eur. J. Med. Chem.*, 2015, **105**, 245–262.
5 R. W. Sidwell, R. K. Robins and I. W. Hillyard, *Pharmacol. Ther.*, 1979, **6**, 123–146.
6 M. D. Mullican, M. W. Wilson, D. T. Conner, C. R. Kostlan, D. J. Schrier and R. D. Dyer, *J. Med. Chem.*, 1993, **36**, 1090–1099.
7 P. Datar and T. Deokule, *Med. Chem.*, 2014, **4**, 390–399.
8 F. Clerici, D. Pocar, M. Guido, A. Loche, V. Perlini and M. Brufani, *J. Med. Chem.*, 2001, **44**, 931–936.
9 H. Foks, D. P. Ksepko and K. Gobis, *J. Heterocycl. Chem.*, 2014, **51**, 507–512.
10 G. Serban, *Molecules*, 2020, **25**, 942.
11 N. Shivakumara and P. M. Krishna, *J. Mol. Struct.*, 2020, **1199**, 126999.
12 P. Skehan, R. Storeng, D. Scudiero, A. Monks, J. McMahon, D. Vistica, J. T. Warren, H. Bokesch, S. Kenney and M. R. Boyd, *J. Natl. Cancer Inst.*, 1990, **82**, 1107–1112.
13 A. Monks, D. Scudiero, P. Skehan, R. Shoemaker, K. Paull, D. Vistica, C. Hose, J. Langley, P. Cronise, A. Vaigro-Wolff, M. Gray-Goodrich, H. Campbell, J. Mayo and M. Boyd, *J. Natl. Cancer Inst.*, 1991, **83**, 757–766.
14 W. M. El-Sayed, W. M. Hussin, A. A. Mahmoud and M. A. AlFredan, *Biomed. Res. Int.*, 2013, **2013**, 1–11.
15 M. A. Ismail, G. A. Abdelwahab, W. S. Hamama, E. Abdel-Latif, F. E. Fardous and W. M. El-Sayed, *Arch. Pharm.*, 2022, e2100385.
16 A. A. Al-Karmalawy, M. A. Dahab, A. M. Metwaly, S. S. Elhady, E. B. Elkaeed, I. H. Eissa and K. M. Darwish, *Front. Chem.*, 2021, **9**, 24–44.
17 H. Y. Aati, A. Ismail, M. E. Rateb, A. M. AboulMagd, H. M. Hassan and M. H. Hetta, *Plants*, 2022, **11**, 2521.
18 M. I. A. Hamed, K. M. Darwish, R. Soltane, A. Chrouda, A. Mostafa, N. M. Abo Shama, S. S. Elhady, H. S. Abulkhair, A. E. Khodir, A. A. Elmaaty and A. A. Al-karmalawy, *RSC Adv.*, 2021, **11**, 35536–35558.
19 K. El-Adl, M.-K. Ibrahim, M. S. Alesawy and I. H. Eissa, *Bioorg. Med. Chem.*, 2021, **30**, 115958.
20 M. S. Alesawy, E. B. Elkaeed, A. A. Alsfouk, A. M. Metwaly and I. Eissa, *Molecules*, 2021, **26**, 6593.
21 M. H. Hekal, F. S. M. Abu El-Azm and S. R. Atta-Allah, *Synth. Commun.*, 2019, **49**, 2630–2641.
22 M. H. Hekal, F. S. M. Abu El-Azm and H. A. Sallam, *J. Heterocycl. Chem.*, 2019, **56**, 795–803.
23 M. A. Yousef, A. M. Ali, W. M. El-Sayed, W. Saber, H. H. Farag and T. Aboul-Fadl, *Bioorg. Chem.*, 2020, **105**, 104366.
24 M. H. Hekal, A. M. El-Naggar, F. S. M. Abu El-Azm and W. M. El-Sayed, *RSC Adv.*, 2020, **10**, 3675–3688.
25 M. S. Salem, R. A. Hussein and W. M. El-Sayed, *Med. Chem.*, 2019, **19**, 620–626.
26 A. M. El-Naggar, A. K. Khalil, H. M. Zeidan and W. M. El-Sayed, *Med. Chem.*, 2017, **17**, 1644–1651.
27 W. A. Hussin, M. A. Ismail, A. M. Alzahrani and W. M. El-Sayed, *Drug Des., Dev. Ther.*, 2014, **8**, 963–972.
28 M. R. Franklin, P. J. Moos, W. M. El-Sayed, T. Aboul-Fadl and J. C. Roberts, *Chem.–Biol. Interact.*, 2007, **168**, 211–220.
29 M. H. Hekal, S. S. Samir, Y. M. Ali and W. M. El-Sayed, *Polycycl. Aromat. Compd.*, 2022, **42**, 7644–7660.
30 W. S. Qayed, M. A. Hassan, W. M. El-Sayed, J. R. A. Silva and T. Aboul-Fadl, *Bioorg. Chem.*, 2022, **126**, 105884.
31 W. M. El-Sayed, T. Aboul-Fadl, J. C. Roberts, J. G. Lamb and M. R. Franklin, *Toxicol. In Vitro*, 2007, **21**, 157–164.
32 S. R. Atta-Allah, A. M. AboulMagd and P. S. Farag, *Bioorg. Chem.*, 2021, **112**, 104923.
33 P. S. Farag, M. M. Hemdan and A. A. El-Sayed, *J. Heterocycl. Chem.*, 2020, **57**, 3428–3441.
34 P. S. Farag, A. M. AboulMagd, M. M. Hemdan and A. I. Hassaballah, *Bioorg. Chem.*, 2023, **130**, 106231.
35 P. S. Farag, M. M. Hemdan and A. I Hassaballah, *RSC Adv.*, 2022, **12**, 10204–10208.
36 M. H. Hekal, P. S. Farag, M. M. Hemdan and W. M. El-Sayed, *Bioorg. Chem.*, 2021, **115**, 105176.
37 S. L. Holbeck, J. M. Collins and J. H. Doroshow, *Mol. Cancer Ther.*, 2010, **9**(5), 1451–1460.
38 A. Lezaja and M. Altmeyer, *Cell Cycle*, 2018, **17**, 24–32.
39 T. C. Tsou, F. Y. Tsai, S. C. Yeh and L. W. Chang, *Arch. Toxicol.*, 2006, **80**, 804–810.
40 M. C. Chang, Y. J. Chen, E. J. Liou, W. Y. Tseng, C. P. Chan, H. J. Lin, W.-C. Liao, Y.-C. Chang, P.-Y. Jeng and J.-H. Jeng, *Oncotarget*, 2016, **7**, 74473–74483.
41 M. Zhang, J. Qu, Z. Gao, Q. Qi, H. Yin, L. Zhu, Y. Wu, W. Liu, J. Yang and X. Huang, *Front. Pharmacol.*, 2021, **11**, 601468.
42 S. A. El-Metwally, A. K. Khalil and W. M. El-Sayed, *Bioorg. Chem.*, 2020, **94**, 103492.
43 A. Arora and E. M. Scholar, *J. Pharmacol. Exp. Ther.*, 2005, **315**, 971–979.

© 2023 The Author(s). Published by the Royal Society of Chemistry

Open Access Article. Published on 25 May 2023. Downloaded on 2/11/2026 2:26:17 AM.
This article is licensed under a Creative Commons Attribution-NonCommercial 3.0 Unported Licence.

44 T. Ozaki and A. Nakagawara, *J. Biomed. Biotechnol.*, 2011, **3**, 994–1013.
45 M. Olsson and B. Zhivotovsky, *Cell Death Differ.*, 2011, **18**, 1441–1449.
46 C. M. Pfeffer and A. T. K. Singh, *Int. J. Mol. Sci.*, 2018, **19**, 1–10.
47 J. Yan, P. Wan, S. Choksi and Z. G. Liu, *Trends Cancer*, 2022, **8**, 21–27.
48 Z. G. Liu and D. Jiao, *Cell Stress*, 2019, **4**, 1–8.
49 D. J. Wood, S. Korolchuk, N. J. Tatum, L. Wang, J. A. Endicott, M. E. M. Noble and M. P. Martin, *Cell Chem. Biol.*, 2019, **26**, 121–130.
50 N. Malhotra, R. Gupta and P. KumarR, *Neurochem. Int.*, 2021, **148**, 105115.
51 L. L. G. Ferreira and A. D. Andricopulo, *Drug Discov. Today*, 2019, **24**, 1157–1165.
52 T. Khan, M. Ali, A. Khan, P. Nisar, S. A. Jan and S. A. Z. K. Shinwari, *Biomolecules*, 2020, **10**, 47.
53 F. Wu, Y. Zhou, L. Li, X. Shen, G. Chen, X. Wang, X. Liang, M. Tan and Z. Huang, *Front. Chem.*, 2020, **8**, 726.
54 D. F. Veber, S. R. Johnson, H.-Y. Cheng, B. R. Smith, K. W. Ward and K. D. Kopple, *J. Med. Chem.*, 2002, **45**, 2615–2623.
55 H. Patel, K. Dhangar, Y. Sonawane, S. Surana, R. Karpoormath, N. Thapliyal, M. Shaikh, M. Noolvi and R. Jagtap, *Arabian J. Chem.*, 2015, **11**, 221–232.
56 A. K. Jain, S. Sharma, A. Vaidya, V. Ravichandran and R. K. Agrawal, *Chem. Biol. Drug Des.*, 2013, **81**, 557–576.
57 A. Tahghighi and F. Babalouei, *Iran. J. Basic Med. Sci.*, 2017, **20**, 613–622.